Journal of
Materials Chemistry B

Materials for biology and medicine

Accepted Manuscript

This article can be cited before page numbers have been issued, to do this please use: A. Torchio, M. Boffito, R. Laurano, C. Cassino, M. Lavella and G. Ciardelli, *J. Mater. Chem. B*, 2024, DOI: 10.1039/D4TB00092G.

ROYAL SOCIETY OF CHEMISTRY

rsc.li/materials-b

Double-crosslinkable poly(urethane)-based hydrogels relying on supramolecular interactions and light-initiated polymerization: promising tools for advanced applications in drug delivery.

Received 00th January 20xx,
Accepted 00th January 20xx

DOI: 10.1039/x0xx00000x

Alessandro Torchio†[a], Monica Boffito†*[ab], Rossella Laurano[a], Claudio Cassino[c], Mario Lavella[d] and Gianluca Ciardelli*[ae]

Physical and chemical hydrogels are promising platforms for tissue engineering/regenerative medicine (TERM). In particular, physical hydrogels are well-suitable to design drug delivery systems due to their reversibility and responsiveness to applied stimuli and external environment. Differently, chemical hydrogels represent the best strategy to produce stable 3D constructs in the TERM field. In this work, these two strategies were combined to develop multi-functional formulations integrating both drug delivery potential with TERM approaches into a single device. Specifically, a novel photo-sensitive poly(ether urethane) (PEU) was developed to form supramolecular networks with α-cyclodextrins (α-CDs). The PEU was successfully synthesized using Poloxamer® 407, 1,6-diisocyanatohexane and 2-hydroxyethyl methacrylate, as assessed by infrared spectroscopy, size exclusion chromatography and proton nuclear magnetic resonance (^{1}H NMR) spectroscopy. Thermo-responsiveness was characterized through critical micellar temperature evaluation and dynamic light scattering analyses which suggested the achievement of a good balance between molecular mass and overall hydrophobicity. Consequently, the formation of supramolecular domains with α-CDs was demonstrated through X-Ray diffraction and ^{1}H NMR spectroscopies. Supramolecular hydrogels with remarkably fast gelation kinetics (i.e., few minutes) were designed at low PEU concentration (≤ 5% w/v). All formulations resulted cytocompatible according to ISO 10993-5 regulation. Noteworthy, mechanical properties and self-healing ability were observed by rheological tests, while fast photo-crosslinking was evidenced (<60 s) by photo-rheology. A high curcumin payload (570 μg ml^{-1}) was encapsulated within the hydrogels, which was released with highly tunable and progressive kinetics in physiological-simulated environment up to 5 weeks. Finally, a preliminary evaluation of printability was performed through an extrusion-based bioprinter obtaining 3D-printed structures showing good morphological fidelity to the original design. Overall, the developed hydrogel platform showed promising properties for application in the emerging field of regenerative pharmacology as (i) easily-injectable drug-loaded formulations suitable for post-application stabilization through light irradiation, and (ii) biomaterial inks for the fabrication of patient-specific drug-loaded patches.

Introduction

Physical hydrogels are extremely interesting systems due to their marked reversibility and processability. Indeed, the main advantage of physically crosslinked networks is represented by the possibility to easily perform injection and adapt them to the external morphologies. High tunability is also another advantage of these systems. Nonetheless, some limitations can be identified. Most importantly, the development of stable and durable hydrogel networks based on physical interactions is challenging. Indeed, a relevant number of weak crosslinks is necessary to properly stabilize a polymeric network in a watery environment. Furthermore, the indispensable hydrophilicity that is required and characterizes these systems induces relevant absorption of fluids from the external environments. Such natural process can lead to a relevant mass exchange with the adjacent milieu and complete dissolution may occur within few days. Although this behavior is ideal for most drug delivery applications, since a relevant number of therapeutic drugs is characterized by high hydrophobicity and low bioavailability and hence needs specific carriers to be delivered, it could represent a strong limitation for the prolonged administration of therapies. This issue is well-known and has been widely discussed by various authors.[1,2]

A possible solution to overcome this drawback can be found in the development of chemically crosslinked hydrogel networks. However, low responsiveness and limited handling are generally correlated to this strategy.[3] Moreover, chemical additives are often necessary to carry out the crosslinking process and hence toxic effects may be induced.[4]

A relatively wider approach consists in the integration of both the physical and chemical crosslinking methods into a single hydrogel formulation with the ultimate goal of combining the advantages of both strategies while reducing related deficiencies. In this regard, a proper selection of the chemical composition and the resulting physical properties are elemental factors to successfully develop hybrid strategies based on both chemical and physical crosslinking. Indeed, the tuning of physical interactions originated by the

[a.] Department of Mechanical and Aerospace Engineering, Politecnico di Torino, Corso Duca degli Abruzzi 24, 10129 Torino, Italy.
[b.] Institute for Chemical-physical Processes, National Research Council (CNR-IPCF), Via G. Moruzzi 1, 56124, Pisa, Italy.
[c.] Department of Science and Technological Innovation, Università del Piemonte Orientale "A. Avogadro", Viale Teresa Michel 11, 15121 Alessandria, Italy.
[d.] Department of Management, Information and Production Engineering, Università degli Studi di Bergamo, Viale G. Marconi, 5, 24044 Dalmine, BG, Italy.
[e.] Department of Life Sciences, University of Modena and Reggio Emilia, Via Campi 287, 41125 Modena, Italy.
† These authors have contributed equally to this work.

Electronic Supplementary Information (ESI) available: ATR-FTIR spectra of P407 and HHP407; CMT curves for HHP407 solutions; DLS volume patterns for HHP407 solutions; ^{1}H NMR spectra of CD-HHP407 complexes; appearance of samples after incubation with DMEM for 24 hours; cytocompatility of CD at different concentrations; appearance of CUR solution in EtOH *vs.* CUR dispersion within CD solution; strain sweep tests to study the self-healing properties of unloaded- and Cur-loaded formulations; rheological frequency sweep tests of CUR-loaded hydrogels; calibration curves used for CUR quantification. See DOI: 10.1039/x0xx00000x

View Article Online
DOI: 10.1039/D4TB00932G

constituent polymeric units in combination with additional chemical crosslinking can result in highly stiff and stable hydrogels, as reported, for example, in the work by Li et al., in which a hydrogel system characterized by an elastic modulus around 5 MPa and a strength equal to 2.5 MPa was described.[5] In detail, the authors discussed how hydrogel network organization and the nature of the occurring interactions account for the development of formulations with remarkable mechanical response. In this work, they developed a hydrogel network stabilized through crystalline (physical) and covalent (chemical) domains using poly(vinyl alcohol) (PVA) to form crystallites and poly(acrylamide) (PAA) to generate chemical bonds. As a result, they obtained a hydrogel system with mechanical properties very similar to the ones of natural tissues, such as cartilage and skin. In this case, chemical crosslinking was pursued through overnight *in situ* polymerization of acrylamide in the presence of N,N'-methylenebisacrylamide (MBAA) and tetramethyl-ethylenediamine (TEMED), at room temperature. Such approach can be considered as a "macromolecular" strategy, in which the organization of the resulting network is based on standard intermolecular interactions.

Nonetheless, a more sophisticated and versatile approach can also be pursued relying on supramolecular (SM) self-assembly. In this case, the initial processability of physical hydrogels is preserved due to the adaptivity of SM networks and a subsequent *in situ* stabilization can be performed through chemical crosslinking. Hence, highly organized SM networks can be *ad-hoc* engineered to exhibit proper functionalities for a further and fast chemical stabilization that induces mechanical strengthening and improves resistance to solubilization. In this regard, the chemical composition of all the components of the deriving hydrogel systems is even more important in terms of tuning and engineering. An interesting example describing this approach can be found in the work conducted by Zhao and co-authors.[6] In this case, a modified di-acryloyl block co-polymer was synthesized using Pluronic® F68 (commercially available also as Poloxamer® 188, P188) and poly(ε-caprolactone) (PCL) with the aim to exploit its photo-sensitivity to ensure fast polymerization after complete self-assembly into poly(pseudo)rotaxanes (PPRs) with α-cyclodextrins (α-CDs).[7-12] The resulting hydrogel systems were characterized by notably high mechanical properties (i.e., storage modulus (G') greater than 100 kPa) and good responsiveness in aqueous environments (i.e., the equilibrium swelling ratio of the developed formulations was dependent over the molar feed ratio of α-CDs to the macromer). Another similar work was conducted by the same authors utilizing the same macromer in the presence of β-CDs, thus further proving the versatility of properly synthesized amphiphilic polymers in enabling the *ad-hoc* engineering of hydrogels best matching the specific requisites of each envisaged application.[13] Differently, Wei and co-workers developed an interesting system composed of star-shaped photo-curable macromers and α-CDs.[14] In detail, they synthesized a methacryloyl-terminated poly(L-lactide)-*b*-poly(ethylene glycol) (PLA-*b*-PEG) copolymer consisting in three or four arms and formulated SM hydrogels by adding α-CDs in aqueous solutions. The presence of photocurable domains was demonstrated to improve the mechanical strength and stability in aqueous environment of the deriving SM networks. Moreover, these systems showed a highly tunable responsiveness in watery environments, reaching swelling ratio values up to 500% within 7 days of incubation in a watery medium. The same research group developed other similar systems based on the same strategy.[15,16]

Although only few research works have focused on the specific design of photo-crosslinkable PPR-based networks over the last decade, the general importance of developing shear-thinning and self-healing hydrogels retaining the potential for a secondary crosslinking has gained a continuously increasing interest. Indeed, the combined possibility to easily process a hydrogel matrix that is intrinsically self-sustaining and then further stabilize it through fast photo-crosslinking also represents an extremely important feature for the development of bioinks and biomaterial inks for extrusion-based 3D printing. The most recent and relevant strategies underpinning this idea have been lately reviewed and critically analyzed by many researchers.[17-19] Specifically, in these publications the authors argued on the key role played by mechanical features in the development of highly effective and functional hydrogel bioinks and biomaterial inks. In this regard, supramolecular-based matrices represent one of the most promising strategies to ensure self-healing and shear-thinning responses, which are elemental features for injection or printing of even cell-laden hydrogels.

Within this scenario and on the basis of the promising results reported in our previous works,[20,21] this work has been conceived with the aim of designing a new platform of double-crosslinkable hydrogels relying of physical SM interactions and chemical bonds resulting from light-initiated radical polymerization. Specifically, in this paper novel SM and photo-curable systems based on a new properly synthesized poly(ether urethane) (PEU) were developed. In fact, *ad-hoc* designed PEUs retain huge potential as forming materials of medical devices due to their *LEGO*-like chemical structure. This peculiarity has been widely exploited in previous studies aiming to properly fulfil various technical and clinical needs.[22-28] In detail, our previous findings indicated Poloxamer® 407 (P407)-based PEUs as the best ones for the formation of PPR-based networks with α-CDs due to their balanced match among molecular mass, hydrophobicity and overall macromolecular functionality induced by chemical domains and structures. Based on these results, a new photo-sensitive PEU based on P407 and 1,6-hexamethylene diisocyanate (HDI) was synthesized by end-capping the pre-polymer chains resulting at the end of the first step of the reaction through the addition of 2-hydroxyethyl methacrylate (HEMA). As a consequence, a further improvement of the gelling ability of the resulting formulations was expected due to a significant reduction of molar mass and a concomitant preservation of the hydrophobic character derived from the partial polymerization reaction. The proposed approach has the advantage of combining into a single polymeric backbone both the potential to form physical hydrogels with α-CDs and the exposure of pendant photo-curable moieties. A complete physico-chemical characterization of the synthesized PEU was performed through Size Exclusion Chromatography (SEC) and Attenuated Total Reflectance – Fourier Transformed Infrared (ATR-FTIR) and Proton Nuclear Magnetic Resonance (^{1}H NMR) spectroscopies. The assessment of PEU thermo-responsiveness was conducted through Dynamic Light Scattering (DLS) analyses and the evaluation of the critical micellar temperature (CMT) of its aqueous solutions. A new platform of photo-curable SM hydrogels was then designed by mixing PEU and α-CDs solutions and the most promising

View Article Online DOI: 10.1039/D4TB00936C

formulations were selected for rheological and photo-rheological characterization, as well as for cytotoxicity evaluation according to the ISO 10993-5 regulation. Curcumin was then encapsulated within these novel PEU-based hydrogels as a notable example of highly hydrophobic (water solubility approx. 3×10^{-8} M)[29] and environment sensitive (poor chemical stability in physiological conditions) drugs.[30-32] Release profiles of curcumin were then obtained from physical and photo-cured hydrogels through incubation in a watery medium in highly destabilizing and physiological-like conditions (i.e., in phosphate buffered saline solution at pH 7.4 and 37 °C). Finally, the suitability of the developed formulations for rapid prototyping was preliminary evaluated through a commercial extrusion-based 3D-printing set-up. Thence, this work was conceived to prove the versatility of PEU synthesis process as an effective tool to produce highly functional and tunable hydrogel systems for potential application as carriers of therapeutic agents in drug delivery, and in the emerging field of regenerative pharmacology.

Experimental section

Materials

Poloxamer® 407 (P407, $\overline{M_n}$ 12,600 Da, 70% w/w poly(ethylene oxide)), 1,6-hexamethylene diisocyanate (HDI), 2-hydroxyethyl methacrylate (HEMA), dibutyltin dilaurate (DBTDL) and 3-(trimethylsilyl)propionic-2,2,3,3-d 4 acid sodium salt (TSP) were obtained from Merck/Sigma-Aldrich (Milan, Italy). α-CDs (from now on simply indicated with the acronym "CDs") and lithium phenyl-2,4,6-trimethylbenzoylphosphinate (LAP, a photo-initiator) were purchased from TCI Chemicals Europe (Zwijndrecht, Belgium). All solvents were purchased from Carlo Erba Reagents (Milan, Italy) in the analytical grade and used as received if not differently stated. Before the synthesis, P407 was dried under mild vacuum (*ca.* 150 mbar) at 100 °C for 8 hours and then kept at 40 °C under vacuum until use. HEMA was dried and stored in a desiccator at low pressure (approx. 1-5 mbar) and room temperature, while 1,2-dichloroethane (DCE) was dehydrated over activated molecular sieves (3 Å, Sigma Aldrich, Milan, Italy) under N_2 flow. HDI was distilled under reduced pressure to completely remove moisture and stabilizers.

Synthesis of the photo-sensitive poly(ether urethane)

The photo-sensitive PEU used in this work was synthesized in two steps according to the protocol reported in our previous works with slight modifications.[21,23,25] In detail, in the first step of the synthesis a prepolymer was produced by reacting P407 (20% w/v) with HDI (2:1 molar ratio with respect to P407) for 2.5 hours at 80 °C in anhydrous DCE under nitrogen atmosphere. Differently, the second step of the reaction consisted in the end-capping of the isocyanate-terminated prepolymer chains through the addition of HEMA (3% w/v in anhydrous DCE, 2:1 molar ratio with respect to P407). The reaction was conducted for 3 hours at room temperature under stirring and protected from any source of light to avoid the occurrence of any side reaction. Then, the reaction was stopped through the addition of methanol to passivate any exposed and unreacted isocyanate group. The solution containing the end-capped PEU was precipitated in petroleum ether (4:1 volume ratio with respect to total DCE volume) at room temperature under vigorous agitation and in the dark. The supernatant was separated from the precipitated PEU, which was kept under a fume hood overnight to allow drying. Subsequently, the dried PEU was solubilized again in DCE at 20% w/v concentration and purified through precipitation in a mixture of diethyl ether and methanol (98:2 v/v, 5:1 volume ratio with respect to DCE volume) in the dark. The purified PEU was collected through centrifugation (Hettich, MIKRO 220R, Tuttlingen, Germany) at 0 °C and 6000 rpm for 20 minutes and dried under a fume hood overnight. The resulting dried polymer was collected and stored under vacuum at 3 °C in the dark until use. The obtained PEU was identified with the acronym HHP407, where the first H refers to the chain extender (HEMA), the second one identifies the diisocyanate (HDI) and P407 indicates the macrodiol.

Physico-chemical characterization of HHP407

Attenuated Total Reflectance – Fourier Transformed Infrared (ATR-FTIR) Spectroscopy. The successful synthesis of HHP407 was demonstrated through ATR-FTIR spectroscopy, which was performed at room temperature on PEU powder utilizing a Perkin Elmer (Waltham, MA, USA) Spectrum 100 Instrument equipped with an ATR accessory with diamond crystal (UATR KRSS). Each spectrum was obtained from 16 scans (4 cm^{-1} resolution) in the spectral domain from 4000 to 600 cm^{-1}. The analysis of data was conducted with the Perkin Elmer Spectrum software. As control sample, the spectrum of P407 was obtained using the same protocol.

Size Exclusion Chromatography (SEC). The molar mass distribution of HHP407 was characterized through an Agilent Technologies 1200 Series (California, USA) SEC equipped with a refractive index detector (RID) and two Waters Styragel columns (HR1 and HR4). N,N-dimethylformamide (DMF, HPLC grade, Carlo Erba Reagents, Milan, Italy) containing LiBr at 0.1% w/v concentration was utilized as mobile phase at a flow rate of 0.4 ml min^{-1}. Registered RID and elution volume data were then exported as .CSV file. Number average molar mass ($\overline{M_n}$), weight average molar mass ($\overline{M_w}$) and dispersity index ($D = \overline{M_w}/\overline{M_n}$) were calculated using Microsoft Excel (Office 365, Microsoft Corporation, USA) and a specific calibration curve obtained from poly(ethylene oxide) (PEO) standards with peak molecular weight (M_p) ranging from 982 to 205,500 Da. For sample preparation, 2 mg of PEU were dissolved in 1 ml of DMF added with LiBr and filtered using poly(tetrafluoroethylene) (PTFE) syringe filters (0.45 μm, LLG International, Meckenheim, Germany).

Proton Nuclear Magnetic Resonance (^{1}H NMR) Spectroscopy. ^{1}H NMR characterization was performed using an AVANCE III Bruker spectrometer equipped with an 11.75 T superconducting magnet (500 MHz ^{1}H Larmor frequency) and a Bruker BVT-3000 unit for temperature control. The NMR spectra were obtained at 300 K after 10 min equilibration at 25 °C. Each spectrum was obtained as the average of 12 scans, with 10 s relaxation time. A sealed capillary containing 1 mM TSP in deuterium oxide (D_2O) was inserted in the NMR tube and used as reference for the zero of the chemical shift

View Article Online
DOI: 10.1039/D4TB00993C

scale. Samples for ^{1}H NMR spectroscopy were obtained through solubilization of HHP407 in D_2O (99.8%, Sigma Aldrich, Italy) at a concentration of 10 mg ml^{-1}. MNova software (Mestrelab Research, S.L, Spain, www.mestrelab.com) was utilized for spectra elaboration.

Investigation of the thermo-responsiveness of HHP407 aqueous solutions

Critical micellar temperature (CMT) evaluation. The evaluation of CMT was carried out to investigate the temperature-dependent behavior of HHP407 aqueous solutions. 1,6-diphenyl-1,3,5-hexatriene (DPH, Sigma Aldrich, Milan, Italy) fluorescent dye (4 x 10^{-4} mol L^{-1} in methanol) was added to PEU solutions (1% w/v concentration) previously prepared in double demineralized water (ddH_2O) or phosphate buffered saline (PBS, pH 7.4, Sigma Aldrich, Milan, Italy) at a final concentration of 2 x 10^{-5} mol L^{-1}. Then, the self-assembly of micelles was studied through an UV-Visible spectrophotometer (Perkin Elmer Lambda 25 UV/VIS spectrometer, Waltham, MA, USA) in the temperature range between 5 and 40 °C at a rate of 1 °C step^{-1} with an equilibration time of 5 minutes step^{-1}. As reported by Boffito et al., [23] the absorbance peak at 356 nm, which is as an indicator of DPH solubilization within the micelle core, was represented as a function of temperature and the CMT value was obtained at the intercept between the linear regions before and after the inflection point that indicates the beginning of the micellization process.[33,34]

Dynamic Light Scattering (DLS). Dynamic light scattering analyses were performed to get additional information of the temperature-driven micellization of HHP407 polymeric chains in aqueous medium. To this aim, HHP407 was solubilized at 1% w/v concentration in ddH_2O or PBS and then analyzed through a Zetasizer Nano S90 (Malvern Instruments, Worcestershire, United Kingdom) instrument. Analyses were conducted at 25 and 37 °C upon sample thermal equilibration at each tested temperature for 5 minutes. Micelle hydrodynamic diameter resulted from the average of three runs. Results are reported as mean ± standard deviation.

Preparation and characterization of HHP407- and CD-based SM complexes

Preparation of supramolecular complexes. The formation of inclusion complexes (ICs) between HHP407 and CDs was evaluated in ddH_2O by mixing their respective solutions. More in detail, concentrated solutions of PEU were produced by solubilizing the total amount of PEU in ddH_2O at 3 °C overnight. Then, a clear solution of CDs at 14% w/v concentration was prepared, added to PEU solutions and the resulting samples were mixed with a vortex (40 Hz, 20-30 seconds). The final samples were characterized by a HHP407 concentration of 1% w/v and the amount of CDs required to theoretically cover the 100% of the available ethylene oxide (EO) domains (i.e., CDs at 7.6% w/v concentration). The samples were incubated for 72 hours at room temperature (i.e., 25 °C) to form ICs. The obtained crystalline matter based on PPR-based complexes was collected through centrifugation (Mikro 220R, Hettich, Germany) at 4500 rpm and 10 °C for 15 minutes. The samples containing SM structures were quenched and frozen using liquid nitrogen and freeze dried (Martin Christ ALPHA 2-4 LSC, Germany) for 24 hours. Hereafter, the obtained SM complexes will be coded as HHP407 1% - SM 100% to indicate that they were designed to theoretically reach a complete coverage of PEO domains through CDs. The recovery of the assembly procedure was estimated according to Equation 1.

$$\text{Recovery } (\%) = 100 - (w_{initial} - w_{final})/w_{initial} \cdot 100 \quad \text{(Eq.1)}$$

where $w_{initial}$ is the initial dried mass of HHP407 and CDs mixed together to produce the inclusion complexes, and w_{final} is the dried mass of the crystalline matter recovered through centrifugation.

^{1}H NMR Spectroscopy. ^{1}H NMR analyses were performed according to the previously described protocol. A SM specimen for ^{1}H NMR spectroscopy was obtained through solubilization of HHP407 1% - SM 100% in D_2O at a concentration of 5 mg ml^{-1}. Spectra of control samples based on CDs and HHP407 as such were also recorded. MNova software (Mestrelab Research, S.L, Spain, www.mestrelab.com) was utilized for spectra elaboration.

X-Ray powder diffraction (XRD) analysis. XRD patterns of HHP407 1% - SM 100% were obtained using an X-Ray diffractometer D5005 assembled with a Bragg-Brentano geometry and vertical goniometer theta - theta (the specimen holder is fixed while tube and detector rotate). The instrument was also equipped with a Ni-filtered Cu Kα (1.542 Å) radiation source set at 40 kV and 40 mA. Tests were performed in step scan mode within the 2θ range from 5° to 30° at increment rate of 0.1° step^{-1} and scan speed of 10 s step^{-1}. As control sample, HHP407 was also analyzed using the same protocol.

Preparation and characterization of HHP407- and CD-based SM hydrogels

Preparation of SM hydrogels. SM hydrogels were produced in Bijou sample containers (17 mm inner diameter, 7 ml volume capacity, Carlo Erba Reagents, Milan, Italy) using PBS (pH 7.4) added with LAP at 0.05% w/v as solvent (PBS/LAP). HHP407 was firstly solubilized in the required amount in PBS/LAP overnight at 3 °C. Then, a clear solution of CDs in PBS/LAP was prepared at 14% w/v and added to HHP407 solutions, thus obtaining gelling systems containing HHP407 at concentration between 1 and 5% w/v and CDs in the 7-10% w/v concentration range. The obtained mixtures were homogenized using a vortex (40 Hz, 30 seconds), while gelation was carried out at room temperature (25 °C). The samples were protected from any source of light during their preparation and characterization to avoid undesired photopolymerization. HHP407-based samples were coded as HHP407 X% - CD Y% where X and Y indicate HHP407 and CD concentrations (% w/v), respectively.

Qualitative evaluation of gelation time and phase-separation in isothermal conditions. Gelation kinetics of SM hydrogels was qualitatively investigated through visual inspection at room temperature (25 °C). In detail, at predefined time steps (i.e., every 1

View Article Online DOI: 10.1039/D4TB00923C

and 5 minutes up to 1 hour observation and then every 10 minutes), the samples (1 ml prepared in Bijou sample containers) were inverted and their flowing along the container's walls was assessed. The condition of "gel" state was characterized by a "no-flow" condition after 30 seconds of vial inversion. Once the gelation process was completed, the samples were maintained at the gelling temperature (25 °C) and visually evaluated every day up to 7 days to assess the occurrence of phase-separation phenomena.

Rheological characterization. Rheological characterization on HHP407-based SM gels was carried out with a stress-controlled rheometer (MCR302, Anton Paar GmbH, Graz, Austria) equipped with a Peltier system for temperature control and a 25 mm parallel plate configuration. Hydrogels were injected through a 5 ml syringe (2 mm tip, *ca.* 0.4 ml) on the lower plate of the rheometer previously equilibrated at 25 °C. The normal force was imposed at 0 N and the thickness of the sample was set at 0.6 mm for all characterizations. Strain sweep tests were carried out at 37 °C and 1 rad s^{-1} angular frequency by sweeping strain values from 0.01 to 500%. The samples that were firstly evaluated through strain sweep test were analyzed again after 15 minutes of recovery in quiescent state and isothermal conditions (37 °C) to characterize hydrogel capability to self-heal after a relevant strain has been applied (i.e., 500%). Frequency sweep tests were performed within the linear viscoelastic region (strain at 0.1%) at 25, 30 and 37 °C and angular frequency from 0.1 to 100 rad s^{-1}.

Self-healing tests were also executed to evaluate the physical reversibility of hydrogels when a cyclic strain was applied over time at 37 °C, according to the protocol described by Wu and co-workers with few modifications.[35] In more detail, a constant strain (0.1%, 1 Hz, recovery phase) was initially applied to the SM hydrogels for 120 seconds; subsequently, a complete rupture of the hydrogel network was caused by the application of a remarkably higher deformation (100%, 1 Hz, rupture phase) for 60 seconds. This cyclic strain was applied on each hydrogel system trice and finally the starting strain (0.1%, 1 Hz, recovery phase) was again applied to estimate the residual mechanical properties of each formulation.

Moreover, due to the photo-responsive nature of HHP407, a photo-rheological characterization was also performed on the same samples. In detail, the storage and loss moduli (G' and G'', respectively) trend of SM hydrogels was registered as a function of time in oscillation (1 Hz, 0.1% strain, 0 N normal force) for 1 minute before UV irradiation. Then, UV light exposure was applied for 1 minute at 365 nm and 10 mW cm^{-2} and the parameters were registered for other 2 minutes in order to assess the overall stability of the photo-crosslinked networks.

Hydrogel biological characterization. To assess the biological compatibility of the designed hydrogels, cell viability and cytotoxicity were both qualitatively and quantitatively evaluated on hydrogel extracts through Live&Dead staining (Invitrogen) and a multiplex assay, respectively. Moreover, the contribution of released CDs on cell metabolic activity was studied by setting up a dose-response test in the concentration range 0 – 10 mg ml^{-1}. For these experiments, NIH-3T3 murine fibroblasts (ATCC® CRL-1658) were regularly cultured in complete medium (i.e., Dulbecco's Modified Eagle's Medium (DMEM, ATCC®) added with MycoZap PLUS (Lonza) antibiotic and 10% v/v Bovine Calf Serum (BCS, ATCC®)) and maintained in a humidified environment at 37 °C, 5% CO_2. Before each experiment, the absence of mycoplasma contaminations was assessed on cell supernatant through the MycoAlert Plus mycoplasma detection kit (Lonza) according to the supplier's instructions.

Preparation of hydrogel extracts and cyclodextrin solutions. Samples for cytotoxicity tests were prepared by weighing 250 mg of self-assembling HHP407-based hydrogels in Bijou sample containers. Three different conditions were tested in order to isolate the contribution of the main features of the hydrogels (i.e., solvent composition and strategy for hydrogel crosslinking), as summarized in Table 1. The samples were acclimatized at 37 °C for 15 minutes, 2.5 ml (i.e., 1 ml every 100 mg of hydrogel) of complete medium (37 °C) were gently added and the systems were incubated for 24 hours at 37 °C. Then, the eluates were withdrawn and collected for the evaluation of cell cytotoxicity and cell viability. Extract sterility was ensured through filtration with 0.22 µm poly(ether sulfone) filters (Carlo Erba Reagents, Milan, Italy).

Table 1 Formulations tested for their biological compatibility.

Sample acronym	Solvent	Physical crosslinking	Chemical crosslinking*
HHP407 X% - CD Y% w/o LAP	PBS	X	
HHP407 X% - CD Y%	PBS/LAP	X	
HHP407 X% - CD Y% UV	PBS/LAP	X	X

* through UV light exposure (365 nm, 10 mW cm^{-2}) for 1 minute

Evaluation of cell cytotoxicity and cell viability. Before cell seeding, 96-well plates were treated to improve cell adhesion. Specifically, gelatin type A (Sigma Aldrich/Merck, Milan, Italy) was first dissolved at 1 mg ml^{-1} in sterile ddH_2O; then, the solution was filtered through 0.22 µm poly(ether sulfone) filters (Carlo Erba Reagents, Milan, Italy) and lastly, it was added to the well plate at 50 µL $well^{-1}$. Subsequently, the plates were incubated at 37 °C for 30 minutes, UV sterilized and finally, they were kept under a sterile cabinet overnight to allow complete water evaporation. Afterwards, NIH-3T3 murine fibroblasts were first collected through trypsinization, re-suspended in complete medium and seeded at 10000 cells $well^{-1}$, as recently reported by Laurano et al.[36] The plates were then incubated in normal culture conditions for 24 h to allow adherence. Subsequently, the medium was removed and replaced with 100 µL of hydrogel extracts or CD solutions and incubated for 24 h. Cell viability/cytotoxicity was first qualitatively assessed through the Live&Dead assay performed following the procedure suggested by the supplier. Briefly, the supernatant was removed and the cells were washed with Dulbecco's Phosphate-Buffered Saline (DPBS). Subsequently, 100 µL of Live&Dead working solution (i.e., 2 µM Calcein AM and 4 µM Ethidium homodimer-1 in DPBS) were added to each well and the plate was incubated for 20 minutes at 37 °C. Lastly, live (green) and dead (red) cells were imaged under a fluorescence microscope (Leica DM IL LED Fluo, Leica Mycrosystems,

View Article Online
DOI: 10.1039/D4TB00982C

Varese, Italy). Cell cytotoxicity was quantitatively investigated by measuring the amount of lactate dehydrogenase released in the medium through CytoTox-ONE™ homogeneous membrane integrity assay (Promega) according to the manufacturer's instructions. Briefly, the 96-well plate was first equilibrated at room temperature for 20 minutes and then, 100 µL of CytoTox-ONE Reagent were added to each well. After 10 minutes of reaction, each well was added with 50 µL of stop solution and lastly, fluorescence was quantified through a multimode plate reader (VICTOR X3, Perkin Elmer) at Ex/Em 535/590 nm. Cell viability was quantitatively evaluated by measuring cell metabolic activity through CellTiter-Blue® cell viability assay (Promega) following the protocols provided by the manufacturer. Briefly, 20 µL of CellTiter-Blue® solution were added to each well and the 96-well plate was incubated at 37 °C, 5% CO_2 for 3 hours. Then, fluorescence was measured through a multimode plate reader (VICTOR X3, Perkin Elmer) at Ex/Em 535/590.

For all the experiments, cells cultured in complete medium and cells treated with a lysing solution were used as negative and positive controls, respectively. Cytotoxicity and cell viability percentages were calculated with respect to the positive and negative control, respectively. Tests were performed in triplicate and results reported as average values ± standard deviation.

Curcumin encapsulation within SM gels, characterization and release studies. A curcumin (Cur) suspension at 1 mg ml^{-1} concentration was prepared in a CD solution at 14% w/v in PBS/LAP. Ultrasound sonication (52 W, 20 kHz, Vibracell VCX130, Sonics, USA) was applied for 3 minutes using a probe and a water-ice bath to avoid evaporation phenomena. The stability of the obtained suspension was evaluated by visual inspection at room temperature (25 °C) in order to define a temporal window for practical use. This suspension was then added to HHP407-based solutions in PBS/LAP thus obtaining SM hydrogels at specific HHP407, CD and Cur contents. Overnight incubation at 25 °C was carried out to ensure complete sample gelation.

The entire set of rheological and photo-rheological characterizations previously described was also conducted on Cur-loaded SM-based hydrogels in order to evaluate the effects of drug loading on the development of SM networks and UV light responsiveness.

SM hydrogels (0.5 ml) for release studies of Cur were prepared in glass vials (10 mm inner diameter, 4 ml volume capacity, Sigma Aldrich, Milan, Italy) and indicated with sample code HHP407 X% - CD Y% Cur, where X and Y indicate PEU and CD concentrations (% w/v), respectively. For all the selected formulations, two sets of 5 samples each were prepared in order to evaluate the behavior of purely physical hydrogel networks and the additional contribution of photo-crosslinking. Upon UV light exposure (1 minute at 365 nm and 10 mW cm^{-2}) samples were identified with the acronym HHP407 X% - CD Y% Cur UV. Release studies were conducted on SM hydrogels at 37 °C after acclimatization for 15 minutes. Then, 1 ml of PBS (37 °C) was gently added on top of each hydrogel sample. At precise time steps (2, 4, 6, 24 hours and 3, 4, 7, 14, 21, 28 and 35 days), eluates were withdrawn and completely refreshed with PBS. Cur quantification was performed through an UV/Vis spectrometer (Perkin Elmer Lambda 25 UV/VIS spectrometer, Waltham, MA, USA) by evaluating the absorbance peak around 430 nm. Reference curves were obtained by specific standard solutions produced through hydrogel dissolution and subsequent dilution (Cur concentration ranging between 1 and 20 µg ml^{-1}).

Extrusion-based 3D printing of SM hydrogels. A preliminary evaluation of the printability of HHP407-based hydrogels was performed utilizing a Cellink Inkredible+ bioprinter (Cellink, USA). The printed CAD design was characterized by a squared grid (15x15 mm) based on two layers (0.45 mm filament diameter and 0.35 mm filament gap). The top view of the resulting geometry is reported in Figure 1. The geometry was obtained utilizing Solidworks 2019 CAD software (Dassault Systèmes SolidWorks Corporation), while Repetier Host v2.1.6 (Hot-World GmbH & Co. KG) was utilized for g-code file generation and optimization. Hydrogel preparation was conducted as reported in the specific section above with slight modifications. In detail, solutions composed of HHP407, CDs and Cur were transferred immediately after mixing (i.e., during gelation) into syringes appositely supplied for the 3D-printer. After overnight incubation at room temperature (i.e., 25 °C), the resulting hydrogel networks were kept at 37 °C and their extrudability was tested with three different syringe tips (200, 250 and 450 µm diameter). Constructs were printed into Petri supports (poly(styrene), 5 cm diameter, Carlo Erba Reagents, Milan, Italy) and analyzed through optical microscopy (Leica DM IL LED, Leica Microsystems, Milan, Italy). Geometrical parameters were estimated through ImageJ software (https://imagej.nih.gov/ij/index.html). Photo-induced crosslinking was performed after the printing procedure utilizing a UV light source at 365 nm (10 mW cm^{-2}). Qualitative evaluation of the stability of 3D-printed structures was carried out through incubation in contact with PBS (pH 7.4, 5 ml) at room temperature (i.e., 25 °C). As a proof of concept of the possibility to use the developed hydrogel formulations as constituents of multi-layered self-standing structures, 25 layers cylinder constructs with a 0/90° pattern were also fabricated (300 µm layer thickness). The hydrogel formulation was prepared as reported above and 3D printed according to the parameters identified through the previously described preliminary extrusion tests. Photo-crosslinking (365 nm, 10 mW cm^{-2}, 30 s/layer) was performed layer-by-layer with the aim of providing the structures with a homogeneous crosslinking density along the Z-axis.

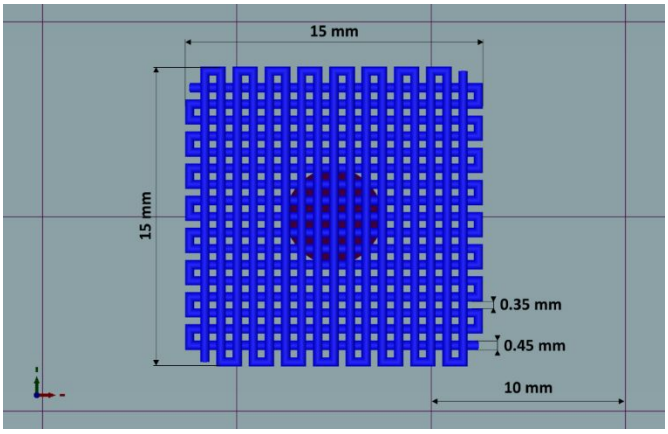

Fig. 1 Top view of the CAD model used to evaluate HHP407-based hydrogel 3D-printability.

View Article Online DOI: 10.1039/D4TB00530C

Statistical Analysis

Statistical analysis was conducted through GraphPad Prism 8 for Windows 10 (GraphPad Software, La Jolla, CA, USA; www.graphpad.com). Two-way ANOVA analysis coupled with Bonferroni multiple comparison test was performed to compare results, assessing the statistical significance according to Boffito et al.[23] Significance level were assigned depending on p-values: *p<0.0001* Extremely significant (****), *0.0001<p<0.001* Extremely significant (***), *0.001<p<0.01* Very significant (**), *0.01<p<0.05* Significant (*), *p≥0.05* Not significant (ns).

Results and discussion

Physico-chemical characterization of HHP407

The ATR-FTIR spectra of HHP407 and P407 are reported in Figure S1. The appearance of the typical vibration bands of urethane domains in HH407 spectrum proved its successful synthesis. In detail, the peak around 1720 cm^{-1} was ascribed to the stretching of C=O domains, while the peak at 1530 cm^{-1} was attributed to the simultaneous bending and stretching of N-H and C-N chemical regions, respectively. Moreover, the typical broad vibrational band around 3350 cm^{-1} was referred to N-H stretching. The absence of signal at *ca.* 2200 cm^{-1} suggested a complete conversion of the isocyanate groups of HDI. In addition, the characterizing vibrational bands of P407 were detected at 1250 cm^{-1} (CH_2 stretching), 2880 cm^{-1} (CH_2 rocking) and 1100 cm^{-1} (C-O-C stretching). Nonetheless, no peaks due to the end-capping molecule (i.e., HEMA) were detectable, probably because they overlapped with peaks related to the macrodiol and in-chain urethane domains. SEC results provided $\overline{M_n}$ equal to 22 kDa and a dispersity index of 1.7. The low D value proved the synthesis of a PEU with a narrow molecular weight distribution as a result of a good control over the polymerization procedure. ^{1}H NMR characterization of HHP407 in D_2O was performed to detect the presence of HEMA domains, thus proving the effectiveness of the end-capping procedure. As reported in Figure 2, the typical peaks of HEMA were detected at 6.15, 5.85 and 1.95 ppm. Moreover, the end-capping procedure turned out to produce polymeric chains containing approximately 1.25-1.5 HEMA units per chain (i.e., up to 75% end-capping yield), when the maximum theoretical value is 2 (i.e., 100% end-capping yield). This result indicated a reliable end-capping reaction during the second step of PEU synthesis. The thermo-sensitive behavior of HHP407-based solutions (1% w/v concentration) was evaluated in PBS and ddH_2O. Figure S2 and S3 reports the CMT curves (i.e., absorbance at 356 nm *vs.* temperature) and the DLS volume patterns, respectively, for HHP407 solutions at 1% w/v concentration. Interestingly, HHP407 solubilized in pure water showed a CMT value of 22.2 °C, while the same formulation prepared in PBS was characterized by a CMT equal to 19.6 °C. This relevant difference can be ascribed to the salting-out effect generated by the presence of dissolved PBS ions in a similar way as for previously studied P407-based PEUs.[21] Interestingly, HHP407 was characterized by comparable CMT values to those of chain extended P407-based PEUs at equal concentration (i.e., 1% w/v), although its molecular mass was significantly lower (i.e., around 30%). The correlation between these results suggested an enhancement in the thermo-induced self-assembly of HHP407 chains into micelles probably originated by a better balance between the overall hydrophobicity and length of the polymer chains. It is also plausible that the presence of end-methacrylate groups could induce a significant contribution in this regard. DLS measurements showed that both the analyzed samples underwent polymer chain organization into micellar structures, with some differences ascribable to the solubilization medium and in particular to the absence of dissolved ions in the sample prepared in ddH_2O. Indeed, at 25 °C the micelle hydrodynamic diameter was measured to be 18.5±5.2 nm and 34.5±3.5 nm for HHP407 solubilized in ddH_2O and PBS, respectively. Irrespective of the solubilization medium, the micelle hydrodynamic diameter increased with increasing temperature at 37 °C, reaching 41.2±7.3 nm and 44.6±5.8 nm for the sample prepared in ddH_2O and PBS, respectively (statistically significant increase for the sample prepared in ddH_2O, *p=0.0118*). Interestingly, polymer solubilization in PBS produced significantly bigger micelles at 25 °C (statistically significant difference, *p=0.0115*), in accordance with the lower CMT value estimated for this sample that thus was able to initiate the micellization process at lower temperature. Conversely, when HHP407 was solubilized in ddH_2O, the same micelle dimension was achieved upon temperature increase at 37 °C (34.5±3.5 nm -HHP407 1% w/v in PBS at 25 °C- *vs.* 41.2±7.3 nm -HHP407 1% w/v in ddH_2O at 37 °C-, not statistically significant difference), in accordance with the higher temperature needed for this sample to initiate polymer chain organization into micellar structures.

Characterization of HHP407-CD SM complexes

The mixture containing HHP407 at 1% w/v and CDs at 7.6% w/v (i.e., 100% theoretical PEO domain coverage, HHP407 1% - SM 100%) in ddH_2O resulted in a 100% recovery (calculated according to Equation 1). This result indicated that HHP407 was a more effective polymer in terms of interaction with CDs in watery environments when compared to previously characterized chain-extended P407-based PEUs, which were characterized by a maximum recovery of 60%.[20,21] Indeed, HHP407 was probably characterized by the best match between molecular mass and resulting hydrophobicity that could enhance its self-assembling ability in forming micelles and thence PPR-based networks in solution. ^{1}H NMR characterization was performed on the resolubilized HHP407 1% - SM 100% crystalline powder to clearly confirm the co-presence of HHP407 and CDs within the collected sample, as reported in Figure S4. In fact, the presence of characteristic peaks of CDs was found within the chemical shift range from 4.05 to 3.55 ppm and at 5.08 ppm, while PEU resonance domains were detected within the chemical shift region between 1.60 and 0.95 and at 3.75 ppm. XRD patterns demonstrated the formation of PPR-based channel-like crystalline structures within HHP407 1% - SM 100% sample, as reported in Figure 3. Indeed, three main peaks at 2θ equal to 7.4°, 12.8° and 19.6° were detected and clearly represented the formation of SM crystals within the HHP407-

View Article Online
DOI: 10.1039/D4TB00092G

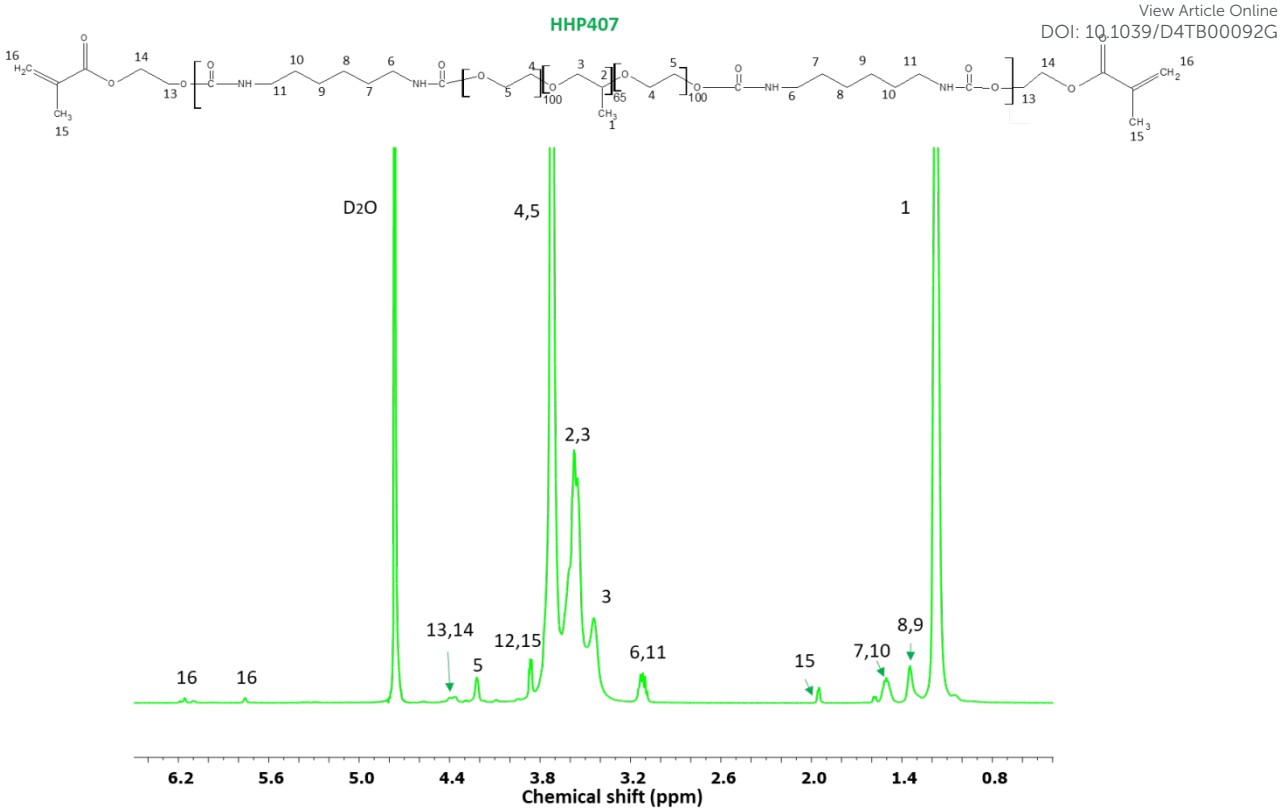

Fig. 2 ^{1}H NMR spectrum of HHP407. All PEU-related proton peaks are indicated by specific numbers and arrows. The presence of typical HEMA domains is indicated by protons 13 and 14 (around 4.2-4.4 ppm), 15 (1.95 ppm) and 16 (5.85 and 6.1 ppm).

based network, as notably indicated in the literature.[37] Instead, the pattern of native HHP407 powders was characterized by the presence of the same peaks that were found in chain extended P407-based PEUs (i.e., at 2θ equal to 19° and 23.3°),[20,21] which were comparable to the ones of P407 sample, thus suggesting that the molecular mass distribution profile and the introduced hydrophobic domains in HHP407 PEU did not influence the crystallization process of the P407 block significantly.

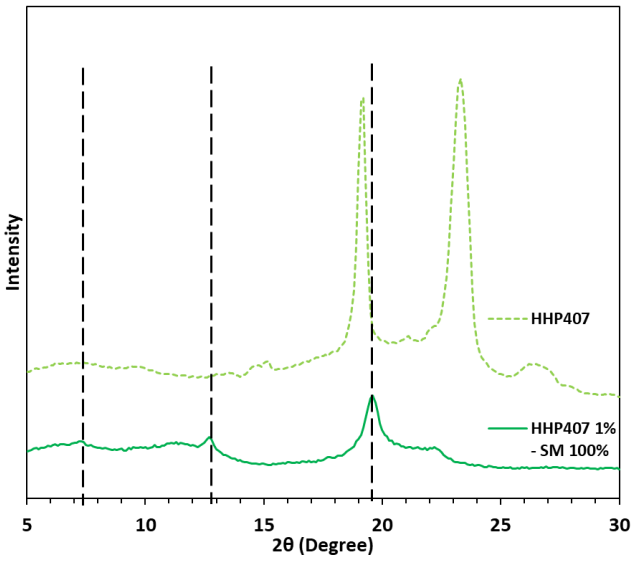

Fig.3 XRD patterns of HHP407 (light green dashed line) and HHP407 1% - SM 100% (green continuous line). Typical peaks of channel-like PPR-based crystals are indicated by black vertical dashed lines at 2θ equal to 7.4°, 12.8° and 19.6°. The pattern of pure HHP407 is also reported for comparative purposes.

Design of HHP407-based SM hydrogels

Gelation properties of SM formulations based on HHP407 and CDs. The high affinity of HHP407 for interaction with CDs clearly indicated that a thorough investigation on hydrogel formulation design would have led to the definition of the best composition for the intended purposes. For this reason, a wide plethora of hydrogel formulations was produced at a maximum PEU content of 5% w/v; gelation time was qualitatively evaluated, as reported in Table 2. Interestingly, no phase-separation phenomena were observed and all the estimated gelation time values were significantly lower with respect to those of identically formulated samples based on other PEUs developed in previous works.[20,21] For instance, HHP407 1% - CD 10% hydrogel sample was characterized by a gelation time around 1 hour and 5 minutes at room temperature (i.e., 25 °C), while an overnight incubation was necessary for identical formulations based on previously characterized PEUs.[20,21] By decreasing CD concentration to 8% w/v, the gelation process was still characterized by extremely fast kinetics. In detail, HHP407 1% - CD 8% required only 4 hours and 20 minutes to result in a turbid hydrogel, while 3 hours were

View Article Online
DOI: 10.1039/D4TB00693C

necessary for HHP407 5% - CD 8%. Thence, HHP407 properties in terms of balance between molecular mass and hydrophobicity (i.e., poly(propylene oxide) (PPO) block dimension and distribution along PEU chains) could be considered as highly effective to enhance the interaction with CDs.

Table 2 Gelation time at 25 °C for SM hydrogel formulations containing HHP407 at 1 and 5% w/v and CDs between 7 and 10% w/v. O.N. = overnight incubation to complete the sol-to-gel transition.

		CDs (% w/v)			
		7	8	9	10
HHP407 (% w/v)	1	O.N.	4h 20'	2h 15'	1h 5'
	5	O.N.	3h	50'	20'

For all the above-mentioned reasons, a selection among these HHP407-based hydrogel formulations was conducted and the hydrogels containing CDs at 8% w/v concentration were selected for further investigations. Such selection was driven by the concurrent possibility to significantly decrease CD content with respect to the previously developed formulations based on chain-extended PEUs (i.e., CD content 20% lower),[21] while keeping gelation relatively fast. Additionally, this novel design would provide clear advantages in terms of hydrogel production-related costs.

Biological characterization of SM hydrogels based on HHP407 and CDs. The biocompatibility of hydrogel extracts was tested according to the ISO 10993-5 regulation. Figure 4a and b show the Live&Dead images and the quantification of released lactate dehydrogenase and cell metabolic activity, respectively, of HHP407 X% - CD 8% samples before and after UV irradiation (sample acronyms HHP407 X% - CD 8% and HHP407 X% - CD 8% UV, respectively). Moreover, the same formulations prepared without the addition of LAP (i.e., HHP407 X% - CD 8% w/o LAP) were also tested to evaluate the effects of the photo-initiator on cell viability. Irrespective of the formulation, all the tested conditions showed a low number of dead cells with respect to the negative control (Figure 4a), thus suggesting a high cytocompatibility of the hydrogel extracts in terms of both system composition and crosslinking process. Indeed, as further quantitatively supported (Figure 4b), no statistically significant differences were observed in cell viability and cytotoxicity percentages of photo-crosslinked samples with respect to their corresponding not-irradiated formulations. On the other hand, both HHP407 1% - CD 8% and HHP407 5% - CD 8% gave slightly lower cell viability values compared to the corresponding LAP-free or photo-crosslinked formulations. Such behavior can be reasonably attributed to the release in the medium of unreacted LAP molecules, which could potentially induce intrinsic cytotoxic effects by interacting with the cells and destroying their membrane. Although cells treated with the extracts deriving from formulations containing 5% w/v HHP407 content showed low cytotoxicity and high cell viability percentages, from a morphological point of view, they appeared round-shaped after 24 h of culture with respect to those treated with lower HHP407 content extracts. Such condition suggested a suffering cell state with reduced cell metabolic activity, as previously assessed for similar PEU hydrogels.[36] However, this evidence cannot be ascribed to effects induced by the release of the polymeric component in the medium. Indeed, systems with 5% w/v HHP407 content are expected to show higher stability compared to those with 1% w/v concentration, in accordance with previous works on similar formulations.[20,21] Furthermore, this behavior was even more evident upon photo-irradiation, thus further supporting this hypothesis, because photo-crosslinked systems were significantly more stable compared to the corresponding physical hydrogels (Figure S5). Conversely, the induction of cell quiescent conditions can be attributed to the release of high amounts of CD. Indeed, as illustrated in Figure S6, the presence of low CD concentrations (i.e., up to 6 mg ml^{-1}) in the medium did not remarkably alter cell viability, but a further increase in CD content progressively led to increased cytotoxicity and reduced cell proliferation. Although the investigated formulations showed the same CD content (i.e., 8% w/v), their interaction with the polymeric counterpart was completely different. More in detail, in systems with HHP407 at 1% w/v concentration, CDs strongly interacted with PEU chains forming PPRs. Conversely, by increasing the polymeric content, the characteristic thermo-responsive behavior of amphiphilic polymers slightly hindered complex formations in favor of micelle arrangement and aggregation. As a result, the amount of CDs involved in the interactions with HHP407 chains was lower in HHP407 5% - CD 8% compared to HHP407 1% - CD 8%, meaning that higher CD contents were free to be released in the medium and thus, induce the slight cytotoxicity we have observed. Nevertheless, both HHP407-based formulations can be considered cytocompatible according to the ISO rules, giving cell viability percentages higher than 70% in all the tested conditions. Hence, these results, in addition to the physical characterization of the hydrogel systems, confirmed their suitability for release tests of Cur in physiological-like conditions.

Characterization of curcumin-loaded SM hydrogels based on HHP407 and CDs

Physical and mechanical characterization. HHP407 1% - CD 8% and HHP407 5% - CD 8% were selected for Cur encapsulation and release tests. In this study, a novel protocol for the production of SM hydrogels containing higher Cur payloads compared to our previous work was optimized.[21] In detail, a solution containing CDs at 14% w/v in PBS/LAP was exploited to suspend Cur at 1 mg ml^{-1} concentration. A homogeneous suspension of Cur was obtained through the aid of ultrasound sonication for 3 minutes under vigorous stirring and the final product is represented in Figure S7. The overall stability of the resulting suspension of Cur- and CD-based complexes was restricted within a temporal range of 30 minutes in static condition at 25 °C; then precipitation phenomena started to occur. Within the temporal frame of stability of the produced Cur suspension, specific aliquots were added to previously prepared HHP407-based solutions in PBS/LAP, thus producing SM hydrogels containing CD at 8% w/v and Cur at 570 μg ml^{-1}. The resulting samples (i.e., HHP407 1% - CD 8% Cur and HHP407 5% - CD 8% Cur) were compared with the corresponding control samples not containing Cur (i.e., HHP407 1% - CD 8% and HHP407 5% - CD 8%). The effects of Cur loading on

View Article Online DOI: 10.1039/D4TB00000C

hydrogel gelation were evaluated through rheological and photo-rheological characterizations. Figure 5 reports the trends of storage and loss moduli (G' and G", respectively) as a function of applied strain (i.e., strain sweep tests). Interestingly, SM hydrogels based on HHP407 at 1% w/v concentration revealed better mechanical properties with respect to formulations at higher PEU content, both in the presence and in the absence of Cur. For example, G' within the linear viscoelastic region (i.e., G'_{LVE}) for HHP407 1% - CD 8% was equal to 6400 Pa, while for HHP407 5% - CD 8% the same parameter was 3800 Pa (i.e., approx. 40% lower than the G'_{LVE} of HHP407 1% - CD 8%). This interesting result could be ascribed to the lower PEU/CD mass ratio that characterized HHP407 1% - CD 8% with respect to HHP407 5% - CD 8%, as hypothesized in previous studies.[20] In that regard, it has been demonstrated that PEU solutions at low concentration (i.e., 1% w/v) are generally characterized by a higher tendency to form supramolecular structures with CDs. This behavior is related to the limited occurrence of aggregate formation in such condition, while at higher PEU content (i.e., 5% w/v) the self-assembly of micellar structures significantly interferes with PPR formation. This hypothesis is in complete accordance with previous studies.[38] The presence of Cur induced a G'_{LVE} decrease of 20% and 26% for formulations containing HHP407 at 1 and 5% w/v, respectively. Moreover, slightly lower critical strain values (γ_L, extreme strain value of the LVE) were observed for the hydrogels containing Cur with respect to the control samples. For example, γ_L value for HHP407 1% - CD 8% was around 0.3%, while for the system containing Cur the same parameter was measured around 0.1%. However, the encapsulation of a notably high payload of Cur (i.e., 570 μg ml^{-1}) did not induce any detrimental effect from a general perspective. Additionally, all the investigated hydrogels showed a relevant self-healing ability (Figure S8). Indeed, G'_{LVE} after complete rupture at 500% strain and recovery in quiescent state at 37 °C for 15 minutes was greater than 88% for all the investigated hydrogel systems. In this regard, hydrogels composed of HHP407 at 1% w/v concentration showed a higher self-healing capacity compared to the formulations at 5% w/v PEU content. Indeed, HHP407 1% - CD 8% systems exhibited recovery values of 97% for the control condition and 93% for the network containing Cur, while for hydrogel systems at 5% w/v HHP407 concentration an 88% recovery was calculated for both cases. This different response could be a consequence of a hindered SM crystallization due to a relevant formation of micelle-based structures within samples containing a higher amount of HHP407 (i.e., 5% w/v), which has been observed to be highly thermo-sensitive through CMT evaluation tests and DLS analyses.

Frequency sweep tests were conducted at 25, 30 and 37 °C with the aim to evaluate the behavior of HHP407-based hydrogels in terms of network development and thermo-responsiveness. All the investigated formulations showed a fully developed gel state at each tested temperature and no cross-over points between G' and G" were identified, as reported in Figure S9. A slight dependence of G' and G" trends over temperature was observed for all the hydrogel systems. For example, even the formulation containing the lowest amount of thermo-sensitive PEU (i.e., HHP407 1% - CD 8%) showed a G' equal to 5700 Pa at 25 °C (at 100 rad s^{-1} applied angular frequency), while the same parameter turned out to be 7400 Pa at 37 °C. Interestingly, the formulation containing HHP407 at 1% w/v showed a better developed hydrogel network with respect to the one containing such PEU at 5% w/v concentration. Indeed, the former was characterized by a less marked dependency of G' and G" over angular frequency compared to the latter. Even frequency sweep tests evidenced better mechanical properties for the hydrogel composed of HHP407 at 1% w/v concentration with respect to the one containing such PEU at 5% w/v. As an example, G' at 37 °C (100 rad s^{-1}) was 7400 Pa for HHP407 1% - CD 8% and 5000 Pa for HHP407 5% - CD 8%. Cur loading induced a slight decrease of the characteristic mechanical parameters, as previously observed and discussed. Cur contribution was more evident in the samples containing HHP407 at 5% w/v with respect to those at 1% w/v PEU concentration, probably because of the presence of a less developed SM hydrogel network at a higher PEU/CD mass ratio (i.e., HHP407 at 5% w/v). However, no significant effects of Cur on hydrogel development were generally observed, since G' and G" of Cur-loaded hydrogels showed consistent trends over applied angular frequency at all the investigated temperatures with respect to control samples. Self-healing tests evidenced a remarkable recovery ability for all the investigated HHP407-based hydrogels, as reported in Figure 6. In fact, a G' recovery greater than 85% after 3 rupture cycles was observed for all the investigated systems. Higher recovery values were measured for samples at 5% w/v HHP407 concentration (i.e., around 95%) with respect to the ones at 1% w/v (i.e., around 88%). This difference could be ascribed to a better fatigue resistance of the hydrogel systems containing the PEU at higher concentration (i.e., 5% w/v), due to a relatively higher damping effect originated by more diffused and interacting amorphous domains[39] (i.e., PEU chains not involved in the formation of SM crystals) with respect to hydrogel networks with lower PEU/CD ratio (i.e., 1% w/v). Indeed, this condition generally favored the organization of the available PEU chains into stiffer PPR-based networks. Finally, the presence of Cur did not significantly affect the mechanical response of the resulting hydrogels to applied rupture cycles and recovery phases. Lastly, photo-rheological tests were performed with the aim to assess the photo-responsiveness of the developed SM hydrogels. In this regard, the typical turbidity of these systems could represent an important impediment to light transmission within the entire hydrogel volume. Nonetheless, all gels showed a good responsiveness to UV light exposure, as highlighted in Figure 7 that reports the trend of complex viscosity (η*) as a function of time during light irradiation. Indeed, the complex viscosity (η*) increased its value during light irradiation for all the tested formulations: a η* increase of *ca.* 16%, 8%, 17% and 12% was measured for HHP407 1% - CD 8%, HHP407 1% - CD 8% Cur, HHP407 5% - CD 8% and HHP407 5% - CD 8%, respectively. A similar trend was also observed for the storage modulus: G' increase after UV light exposure was quantified around 19% and 17% for HHP407 1% - CD 8% and HHP407 5% - CD 8% hydrogels, respectively.

View Article Online
DOI: 10.1039/D4TB00092G

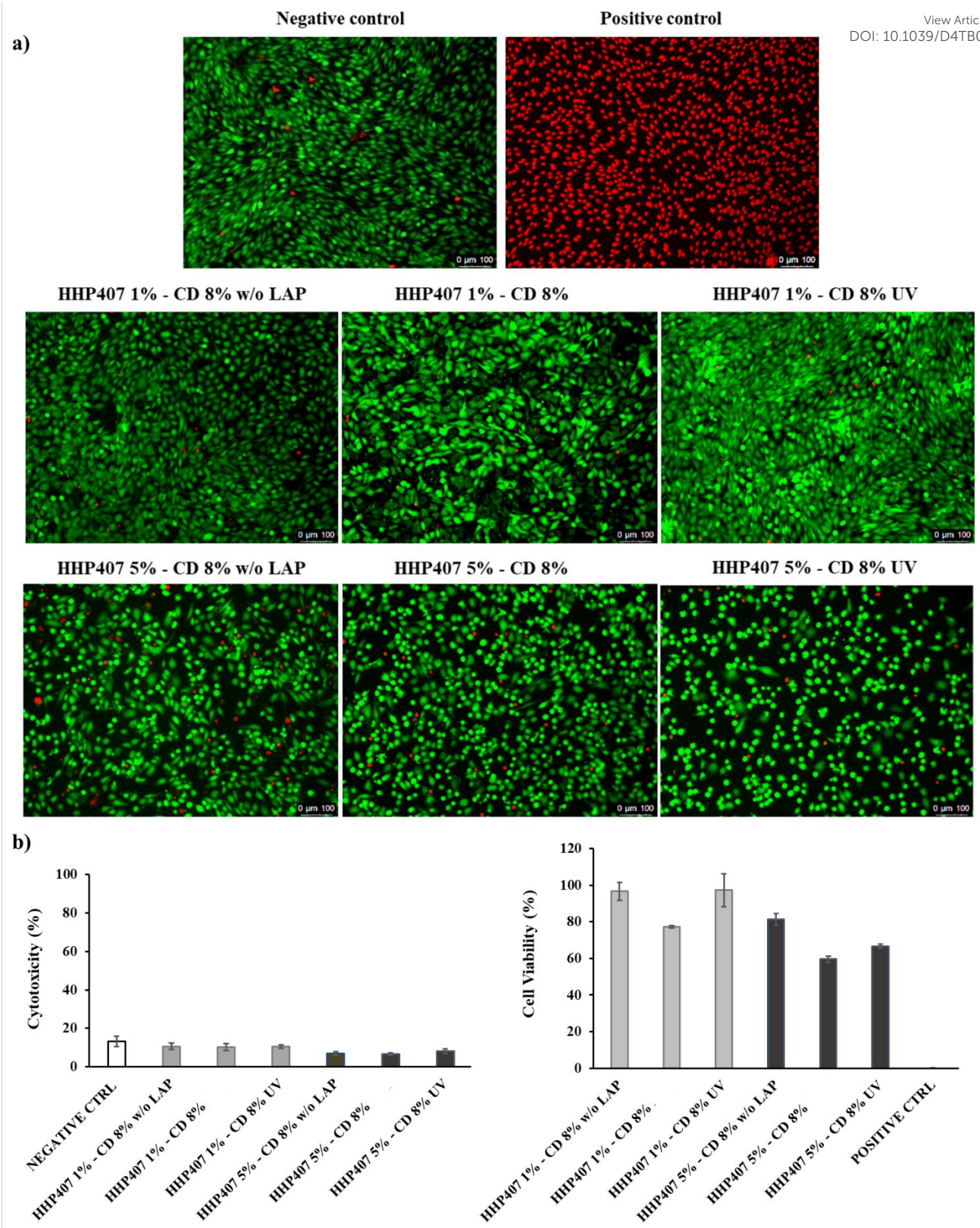

Fig. 4 a) Live&Dead images of NIH-3T3 murine fibroblasts treated with HHP407 X% - CD 8% based extracts after 24h of incubation in normal culture conditions. Live and dead cells are stained in green and red, respectively. **b)** Evaluation of NIH-3T3 cytotoxicity and cell viability induced by HHP407 X% - CD 8% based extracts prepared according to the ISO 10993-5 rules and tested through CytoTox-ONE™ and CellTiter-Blue assays, respectively.

View Article Online
DOI: 10.1039/D4TB00092G

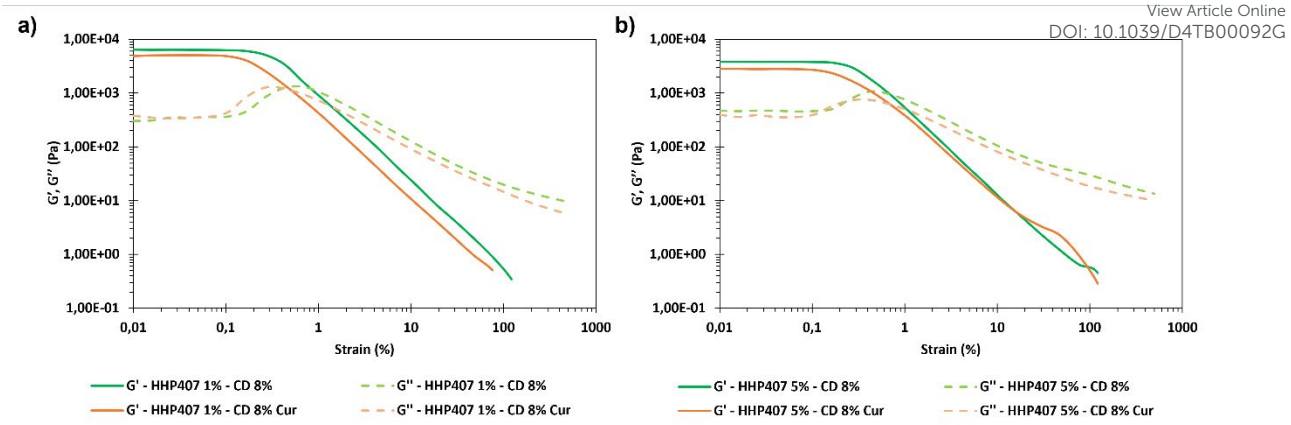

Fig. 5 G' (continuous lines) and G" (long dashed lines) trends as a function of applied strain at 37 °C for **a)** HHP407 1% - CD 8% (green) and HHP407 1% - CD 8% Cur (orange), and **b)** HHP407 5% - CD 8% (green) and HHP407 5% - CD 8% Cur (orange).

Differently, an 8% and 11% G' increase was observed in average for hydrogel systems containing Cur at 570 µg ml^{-1} and PEU at 1 and 5% w/v concentration, respectively. These results suggested a lower photo-curing potential for Cur-loaded systems due to the typical Cur photo-sensitivity that provided a contribution in terms of UV light dissipation. Interestingly, the visual inspection of the sample containing HHP407 at 1% w/v and Cur indicated a significant reduction of the original intense orange color. This observation indicated an indisputable degradation of a relevant amount of Cur payload within the hydrogel network containing PEU at low concentration. Differently, no significant color changes were observed for HHP407 5% - CD 8% samples, thus suggesting that the higher content of photo-sensitive PEU helped in the preservation of the Cur payload. Such behavior could be ascribed to two main aspects. First, a significantly higher number of photo-sensitive groups was intrinsically present in the formulation containing HHP407 at 5% w/v compared to 1% w/v, thus competing with Cur degradation process in terms of UV light absorbance through the formation of chemical crosslinks. Second, it could be likely that a higher content of PEU could help in terms of Cur stabilization and protection from degradation through its encapsulation into the more available hydrophobic domains. In conclusion, the performed photo-rheological characterization suggested that a shorter UV light exposure could be sufficient to achieve complete crosslinking and this aspect was particularly relevant for the samples containing HHP407 at low concentration (i.e., 1% w/v). More specifically, the results suggested that an almost complete crosslinking was obtainable within 20-30 seconds of UV light irradiation for all the investigated hydrogels, as observable from the complex viscosity curves reported in the graphs in Figure 7.

Release profiles of Cur encapsulated within HHP407-based hydrogels. Release studies were performed on Cur-loaded SM hydrogels subjected to just physical crosslinking (acronym HHP407 X% - CD 8% Cur) or to the double crosslinking process (i.e., physical + chemical crosslinking) (acronym HHP407 X% - CD 8% Cur UV). The quantification of the released drug was conducted using specific calibration curves based on standard samples prepared from a stock solution obtained by re-solubilizing the hydrogel systems in PBS. Such procedure was necessary in this case because the high amount of encapsulated Cur (i.e., 570 µg ml^{-1}) induced a highly more important contribution of the involved PEU in terms of solubilization and delivery of the drug with respect to our previous study where PEU content ranged within 1 and 3% w/v and Cur was loaded at 80 µg ml^{-1}.[21] In this study, the involvement of specific PEU-dependent structures was hypothesized, as suggested from the available literature on the design of Cur-loaded systems based on amphiphilic polymers.[40,41] Calibration curves obtained from HHP407 1% - CD 8% and HHP407 5% - CD 8% samples are reported in Figure S10. Totally different calibration curves were obtained, although the only difference between these samples was related to PEU content. In detail, a higher molar extinction coefficient was estimated for the system containing HHP407 at 5% w/v with respect to that at 1% w/v PEU concentration, indicating a likely enhanced Cur integration and solubilization at higher PEU concentration. Moreover, notably good linear fittings were calculated.

Cur release profiles from all hydrogels (i.e., HHP407 1% - CD 8% Cur, HHP407 1% - CD 8% Cur UV, HHP407 5% - CD 8% Cur, HHP407 5% - CD 8% Cur UV) showed significantly different trends, which were correlated to hydrogel formulation and crosslinking method, as shown in Figure 8. Generally, the systems exposed to UV light showed delayed delivery of Cur and were able to sustain this process up to 35 days of incubation in physiological-like conditions (i.e., in contact with PBS at 37 °C). Surprisingly, the entire payload of Cur (i.e., 285 µg/sample) was released also from UV-cured systems, thus indicating an optimal preservation of its chemical stability within the SM networks, which indeed acted as protective element for such highly sensitive drug. Interestingly, SM hydrogels based on HHP407 at 1% w/v concentration exhibited a slower release kinetics compared to those containing such PEU at 5% w/v concentration. In particular, at each time point a significantly higher release rate was observed for HHP407 5% - CD 8% Cur UV with respect to HHP407 1% - CD 8% Cur UV (data not shown, $p < 0.0012$). This observation could be correlated to the previous rheological and photo-rheological characterizations, in which the hydrogels composed by HHP407 at 1% w/v concentration showed the highest G' values, thus indicating the formation of highly rigid networks, due to an enhanced SM self-assembly into PPR-based crystals.[42,43]

View Article Online
DOI: 10.1039/D4TB00092G

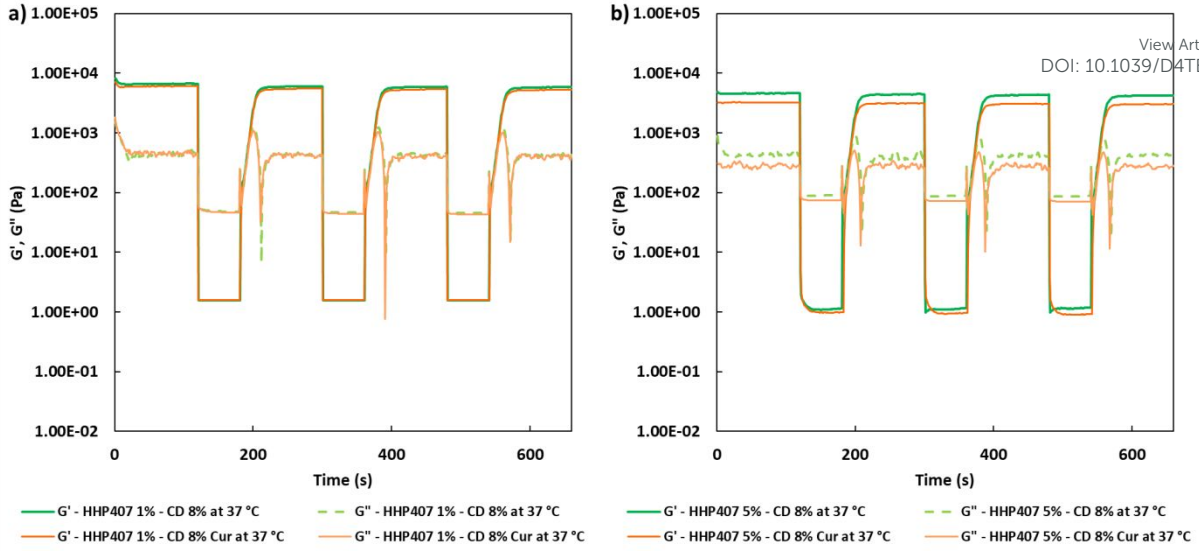

Fig. 6 Strain test curves reporting the trends of G' (continuous lines) and G" (dashed lines) as a function of time during cyclic rupture (100% strain, 60 seconds) and recovery (0.1% strain, 120 seconds) of hydrogel networks at **a)** 1% and **b)** 5% w/v HHP407 concentration at 37 °C. Control hydrogels (green lines) are compared to the ones containing Cur at 570 μg ml^{-1}(orange lines).

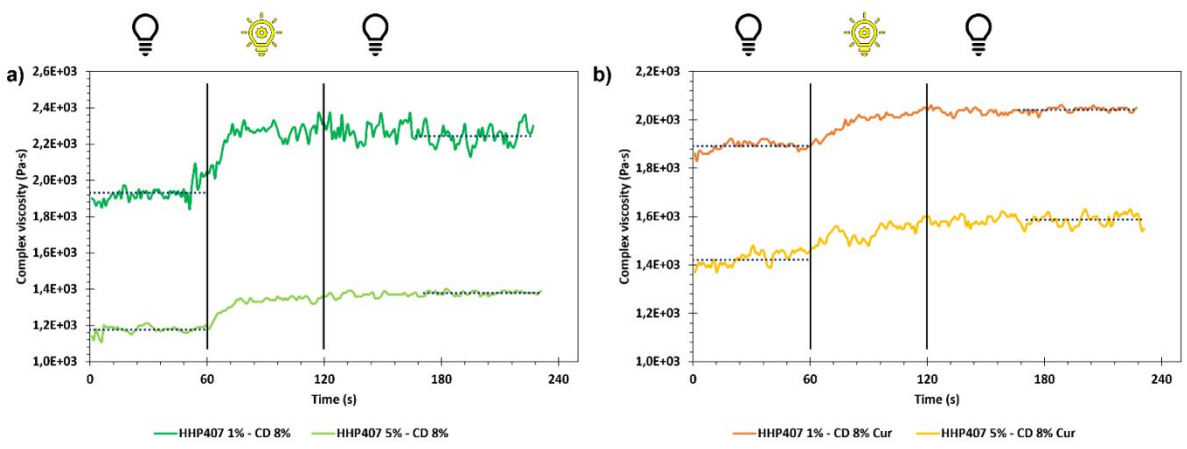

Fig. 7 Complex viscosity trends as a function of time for hydrogels **a)** at 1 and 5% w/v HHP407 concentration as such, and **b)** containing Cur at 570 μg ml^{-1}. Hydrogels were characterized before photo-crosslinking for 60 seconds. Then, exposure to UV light (365 nm, 10 mW cm^{-2}) was conducted for 60 seconds and the resulting mechanical properties were registered for additional 120 seconds. Horizontal dotted blue lines identify the mean complex viscosity values in before (in the first 60 seconds of observation) and after photo-curing (in the last 60 s of observation).

Even in this case, the characterizing PEU/CD ratio suggested the formation of differently organized networks that were also able to undergo photo-induced crosslinking and open the way towards the possibility to finely tune the resulting release kinetics.

Preliminary studies on HHP407-based SM hydrogel extrudability and printing.

In this study, a preliminary evaluation of the general printability of HHP407-based hydrogel systems was conducted. The formulation HHP407 5% - CD 8% was selected to this purpose due to its lower rigidity and generally higher damping/self-healing ability that were observed through rheological characterizations. These parameters are fundamental aspects to consider for the selection of a potential bio-ink or biomaterial ink.[44] The printing process was conducted by controlling different parameters: tip extrusion diameter (D_E), extrusion pressure (P_E), printhead velocity (v_P), syringe temperature (T_s), and bed temperature (T_B). The printing process was conducted at 37 °C for both the syringe and bed in order to favor the stabilization of the hydrogel network through a major contribution of the hydrophobic interactions. A preliminary set of optimized parameters was obtained and reported in Table 3.

Table 3 Selected parameters for the printing process.

D_E	P_E	v_P	T_s	T_B
250 μm	35-40 kPa	10 mm s^{-1}	37 °C	37 °C

Figure 9 reports the produced 3D-printed constructs and a qualitative comparison between the resulting geometry and the theoretical CAD design. The printing process produced constructs with good definition and acceptable printing fidelity. In fact, filament

View Article Online
DOI: 10.1039/D4TB00092G

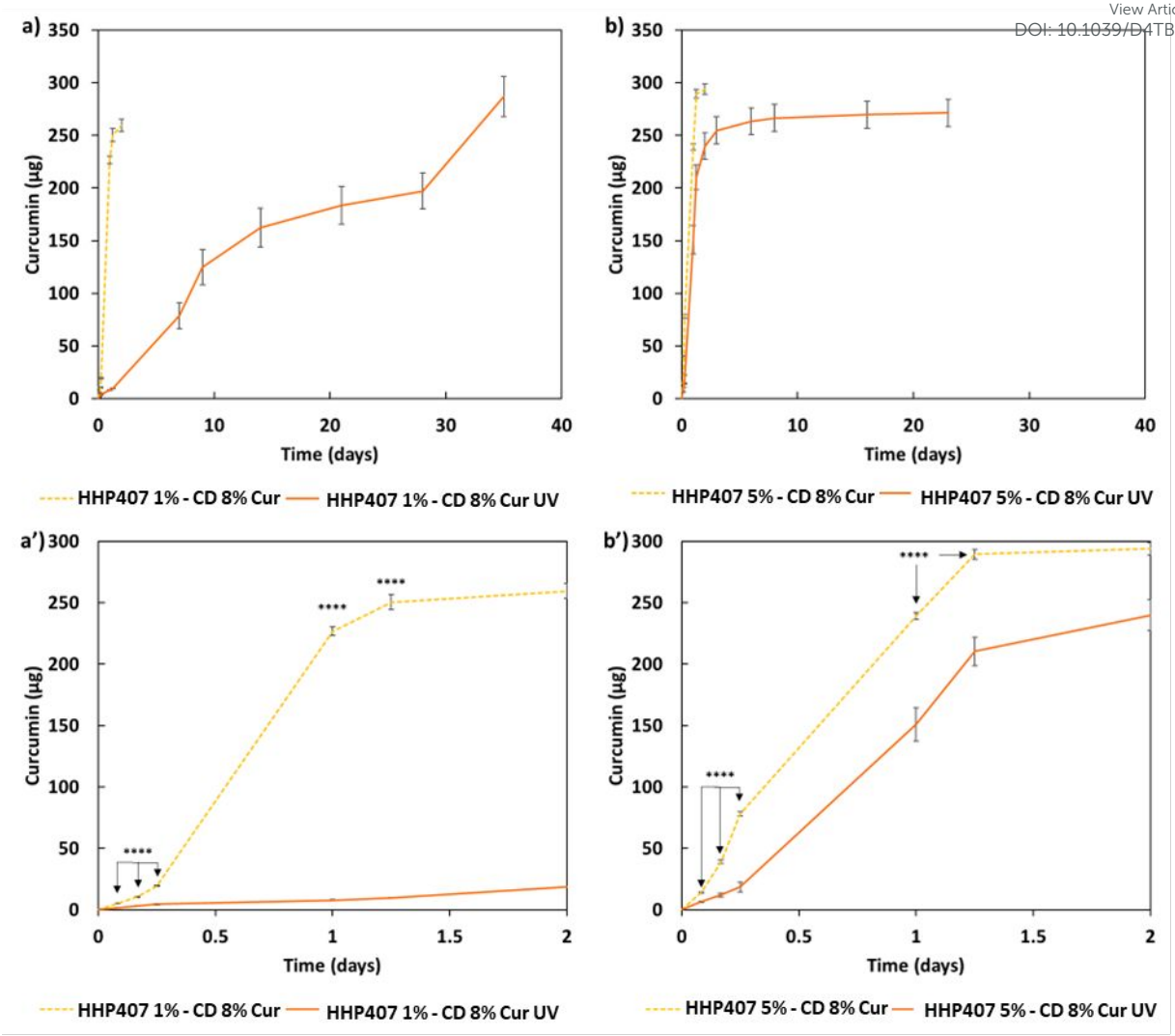

Fig. 8 Cur release profiles from hydrogel systems in contact with PBS at 37 °C and characterized by different HHP407 contents: **a,a')** 1% w/v (HHP407 1% - CD 8% Cur and HHP407 1% - CD 8% Cur UV) and **b,b')** 5% w/v (HHP407 5% - CD 8% Cur and HHP407 5% - CD 8% Cur UV). Physical hydrogels (light orange dashed lines) are compared with photo-cured systems (orange continuous lines). a') and b') graphs represent in detail the release profile measured within the first 2 days of observation.

diameter turned out to be 0.46 ± 0.08 mm (average of 5 measurements obtained from 4 different filaments), while the theoretical value was 0.45 mm, thus proving extrudability and filament formation. The selection of a smaller tip diameter (0.25 mm) with respect to the theoretical value (0.45 mm) was driven by the need to reach the best compromise between printing velocity and required extrusion pressure. Indeed, in the selected conditions, the production of two layers grids with a 0/90° pattern required an overall printing time of around 1 minute. Pore dimension was larger than the theoretical design: the calculation of the pore area of the printed constructs resulted to be 0.17 ± 0.04 mm^2, that is around 40% higher than the theoretical one. This difference could be ascribed to defects in proximity of the intersections between the two layers. Nonetheless, a general good printability could be deduced from these preliminary results. Further optimization could be done based on geometry investigation through more precise methodologies (e.g., computed tomography or optical coherence tomography) in order to better find the correlation between morphological features and printing parameters. Another qualitative characterization was conducted in terms of stability in contact with a large volume of an aqueous medium (PBS, 5 ml, 25 °C) (Figure 10). UV cured systems (HHP407 5% - CD 8% Cur UV) showed a significantly improved residence time in aqueous medium with respect to the physically-crosslinked sample (HHP407 5% - CD 8% Cur). In fact, as shown in Figure 10, the UV light-irradiated samples preserved their geometrical integrity up to 3 days of observation in a highly destabilizing aqueous environment, while physically-crosslinked samples were completely solubilized within an incubation time of 3 hours.

View Article Online
DOI: 10.1039/D4TB00092G

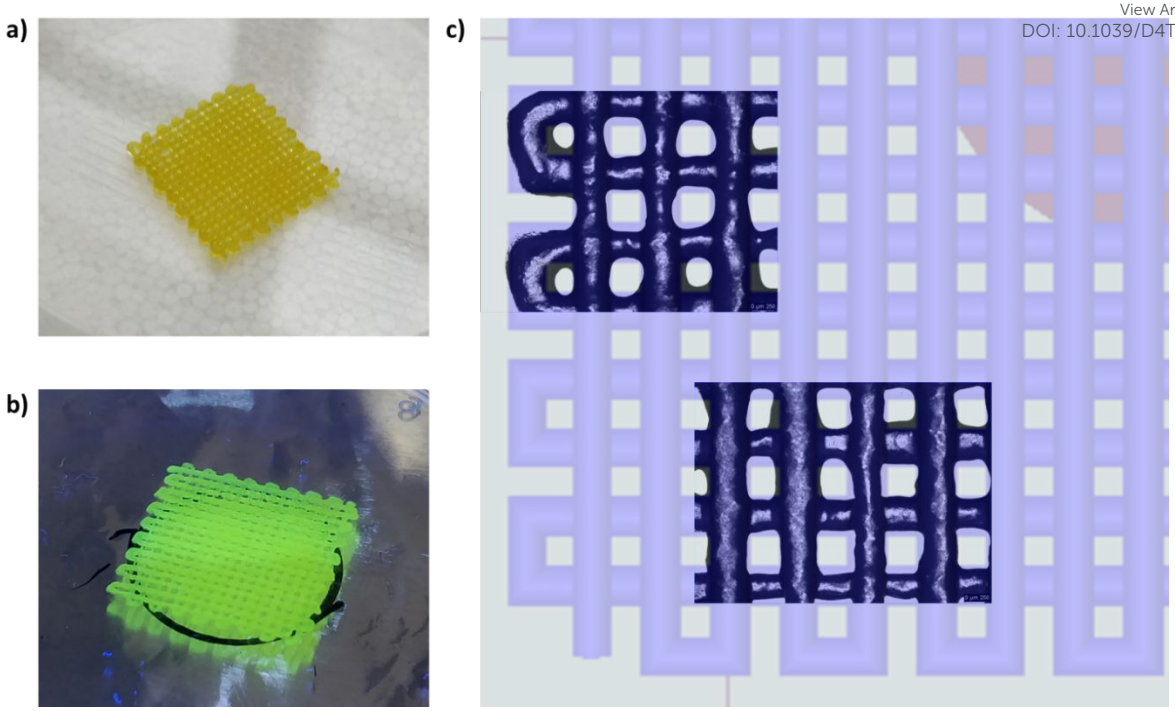

Fig. 9 ***a)*** *Photo of a 3D-printed construct based on HHP407 5% - CD 8% Cur,* ***b)*** *UV curing of HHP407 5% - CD 8% Cur structures,* ***c)*** *Qualitative geometrical match between the 3D-printed HHP407 5% - CD 8% Cur and the starting theoretical CAD design.*

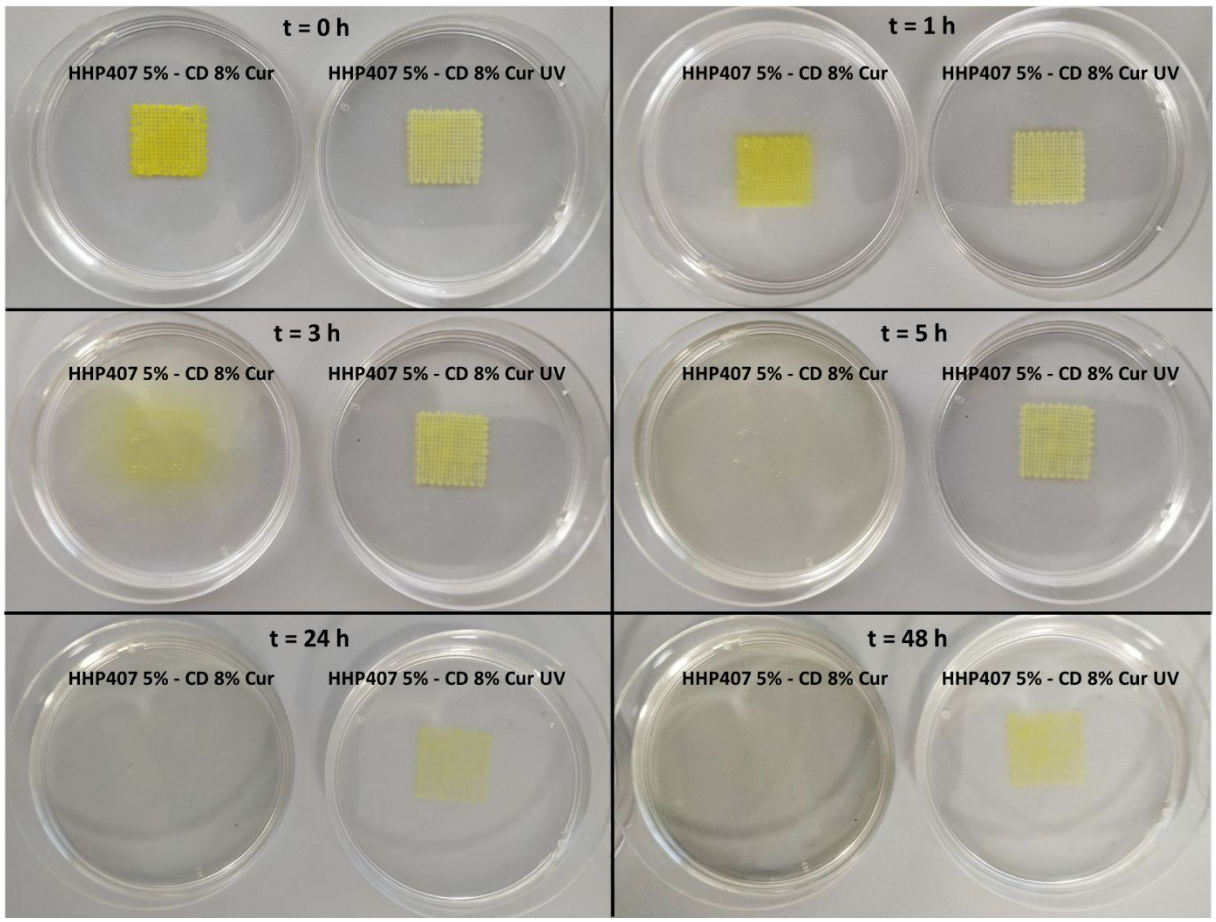

Fig. 10 *Qualitative evaluation of stability for 3D-printed HHP407 5% - CD 8% Cur and HHP407 5% - CD 8% Cur UV structures in contact with 5 ml of PBS at 25 °C (within a Petri support - 50 mm diameter).*

Moreover, an evident color change was observed after UV curing for 1 minute, thus indicating that the resulting relevant interfacial surface and the limited thickness of the construct probably enhanced the exposure of Cur to photo-degradation. Nonetheless, an evident yellowish color was maintained, indicating a relevant protective effect of HHP407 and CDs on Cur even in such particularly degradative conditions. Indeed, the same UV curing protocol applied to the samples utilized for Cur release studies did not induce any evident degradation phenomena, due to the concurrent protective effect provided by HHP407/CDs and the selected sample geometry (i.e., thickness, overall volume). Lastly, the HHP407 5% - CD 8% hydrogel formulation was successfully used to print 25 layers (300 µm layer thickness) cylinder constructs with a 0/90° pattern. The layer-by-layer photo-curing process effectively stabilized each 3D printed layer, resulting in a self-standing construct with a final height of *ca.* 0.75 mm, in agreement with the expected theoretical one. Figure 11 reports the macroscopic appearance of the 3D printed structures during fabrication (Figure 11a) and at the end of the printing process, highlighting the absence of evident structure collapse and consequent pore closing phenomena (Figure 11b).

Conclusions

In this work, a novel photosensitive PEU was synthesized implementing a modification of a well-known and optimized synthesis process.[21,23,25] Indeed, HHP407 PEU was synthesized by using HEMA as end-capping alcohol of the isocyanate-terminated prepolymer chains resulting from the prepolymerization reaction between P407 and HDI.

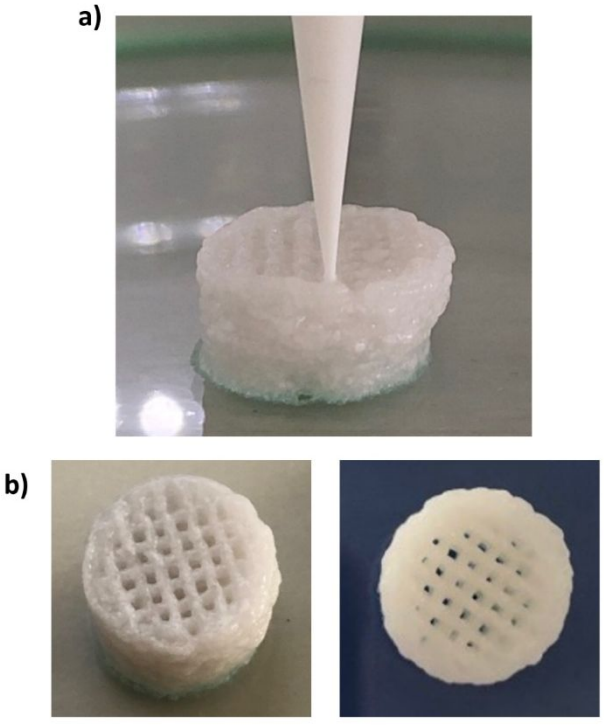

Fig. 11 ***a)*** *Photo of a HHP407 5% - CD 8%-based 25 layers cylinder construct with a 0/90° pattern taken during the 3D printing process,* ***b)*** *macroscopic appearance of 3D printed 25 layers cylinder constructs with a 0/90° pattern at the end of the printing process.*

A complete physico-chemical characterization indicated a good functionalization of the resulting PEU chains through the exposure of methacrylate end-groups. Moreover, a notably good thermo-sensitivity was assessed by CMT evaluation and DLS analyses, although HHP407 lower molecular mass compared to chain-extended 407-based PEUs already developed by our group.[21] This behavior suggested the achievement of a well-balanced polymer structure and hydrophobicity in terms of length and distribution of the available domains (i.e., PPO, HDI and probably also HEMA). Because of the resulting physico-chemical properties, HHP407 turned out to be suitable for the formation of PPR-based crystals in aqueous environment. Moreover, it resulted to be a particularly proper polymer for the formation of SM networks among the whole plethora of materials investigated in literature.[21,43] Thence, it is likely that its structural features represented an optimized set of properties for constructive interaction with CDs, resulting in highly stable and simultaneously responsive networks. This particular behavior allowed the design of SM hydrogels with good mechanical properties at low HHP407 content (i.e., ≤5% w/v) and a relatively low CD concentration (i.e., 8% w/v). In this regard, the formulation showing the lowest PEU/CD mass ratio (i.e., 1% and 8% w/v HHP407 and CD concentration, respectively) was characterized by better mechanical properties with respect to the system containing HHP407 at 5% w/v, as assessed through rheological characterizations. This observation was in evident agreement with the previous results obtained for similar systems, thus further reinforcing the hypothesis of the high functionality and tunability of PEU macromolecules at low concentrations in combination with CDs.[20,21] Although HHP407 produced highly crystalline hydrogel networks with CDs, with the consequent possibility of obtaining brittle hydrogels, a notorious self-healing ability was even observed. Photosensitivity was assessed by means of photo-rheological characterizations. Irrespective of HHP407 and CD content, all tested formulations (i.e., purely physical hydrogels, and both physically and chemically crosslinked hydrogels) showed high cytocompatibility according to the ISO 10993-5 regulation. Cur delivery studies evidenced that hydrogel composition and consecutive photo-crosslinking play a key role in tuning Cur release kinetics from HHP407-based networks. Furthermore, Cur *in vitro* release tests demonstrated the protective ability of HHP407 and CDs on this photo-sensitive drug, opening the way to the possibility to sustain the release of Cur in aqueous environments up to 5 weeks. Interestingly, these samples did not show any color change upon light irradiation, resulting in the possibility to completely release the encapsulated Cur payload. Conversely, under different experimental set-up (i.e., lower sample thickness and higher exposed surface area), we observed a slight color change of the samples (higher for samples with lower PEU content and thus lower polymer induced Cur protection) suggesting the occurrence of Cur photo-induced degradation. Overall, our data suggest that depending on the geometrical features of the developed construct (e.g., 3D bioprinted structure or injected deposit filling a cavity), a fine optimization of the polymerization process should be performed (e.g., by minimizing the irradiation time) to protect the loaded Cur molecules from photo-induced degradation. Finally, one formulation among the developed hydrogels was preliminary evaluated for the production of 3D-printed structures with good resolution. Such

results further indicated HHP407 as a highly versatile polymer for the development of engineered devices for regenerative medicine. Hence, this study confirmed the great potential of properly synthesized PEUs as raw materials for the design of SM hydrogels at low synthetic polymer content, and showing good mechanical performances, progressive release profiles of encapsulated drugs, and easy processability through extrusion-based 3D bioprinting. The observed properties open the way towards future insights into the use of the here-described hydrogel platform for 3D cell culture[45], inject-based bioprinting[46] and vat-polymerization 3D bioprinting[47] among others. Overall, we can conclude that the developed hydrogels can find widespread application in the emerging field of regenerative pharmacology, as (i) easily injectable drug-loaded systems suitable for a perfect filling of body defects through a mini-invasive procedure, and (ii) drug-loaded biomaterial inks in the fabrication of patient-personalized patches. Hence, the here designed hydrogels hold great promise that warrants their further development and characterization in future investigations targeting specific applications in the biomedical field (e.g., wound healing, endodontics, cartilage repair).

Author Contributions

Alessandro Torchio: Conceptualization, Methodology, Validation, Formal analysis, Investigation, Data curation, Writing - original draft, Visualization. **Monica Boffito**: Supervision, Resources, Conceptualization, Methodology, Validation, Investigation, Writing - review & editing, Funding acquisition, Visualization. **Rossella Laurano**: Methodology, Investigation, Data curation, Writing - original draft. **Claudio Cassino**: Investigation, Data curation, Writing - review & editing. **Mario Lavella**: Investigation, Data curation, Writing - review & editing. **Gianluca Ciardelli**: Supervision, Resources, Writing - review & editing, Funding acquisition.

Conflicts of interest

The authors declare that they have no known competing financial interests or personal relationships that could have appeared to influence the work reported in this paper.

Acknowledgements

The research leading to these results has received funding from the European Union - NextGenerationEU through the Italian Ministry of University and Research under PNRR - M4C2-I1.3 Project PE_00000019 "HEAL ITALIA" to Gianluca Ciardelli CUP E93C22001860006 of University of Modena and Reggio Emilia.

Part of this study was carried out within the Ministerial Decree no. 1062/2021 and received funding from the FSE REACT-EU - PON Ricerca e Innovazione 2014-2020.

The views and opinions expressed are those of the authors only and do not necessarily reflect those of the European Union or the European Commission. Neither the European Union nor the European Commission can be held responsible for them.

References

1 R. Eelkema, A. Pich. *Adv. Mater.* 2020, **32**, 1906012.
2 W. Hu, Z. Wang, Y. Xiao, S. Zhang, J. Wang. *Biomater. Sci.* 2019, **7**, 843–855.
3 B. Tian, S. Hua, Y. Tian, J. Liu. *J. Mater. Chem. B* 2020, **8**, 10050–10064.
4 Y.S. Zhang, A. Khademhosseini. *Science* 2017, **356**, eaaf3627.
5 J. Li, Z. Suo, J.J. Vlassak. *J. Mater. Chem. B* 2014, **2**, 6708–6713.
6 S.P. Zhao, L.M. Zhang, D. Ma, C. Yang, L. Yan. *J. Phys. Chem. B* 2006, **110**, 16503–16507.
7 A. Harada, M. Kamachi. *Macromolecules* 1990, **23**, 2821–2823.
8 J. Li, A. Harada, M. Kamachi. *Polym. J.* 1994, **26**, 1019–1026.
9 X. Li, J. Li. *J. Biomed. Mater. Res. A* 2008, **86**, 1055–1061.
10 E. Larrañeta, J.R. Isasi. *Langmuir* 2012, **28**, 12457-12462.
11 J. Li, X. Ni, Z. Zhou, K.W. Leong. *J. Am. Chem. Soc.* 2003, **125**, 1788–1795.
12 X. Ni, A. Cheng, J. Li. *J. Biomed. Mater. Res. A* 2009, **88**, 1031–1036.
13 S.P. Zhao, W.L. Xu. *J. Polym. Res.* 2010, **17**, 503–510.
14 H. Wei, A.Y. Zhang, L. Qian, H. Yu, D. Hou, R. Qiu, Z.G. Feng. *J. Polym. Sci. A Polym. Chem.* 2005, **43**, 2941–2949.
15 H. Wei, H. Yu, A. Zhang, L. Sun, D. Hou, Z. Feng. *Macromolecules* 2005, **38**, 8833–8839.
16 H. Wei, J. He, L. Sun, K. Zhu, Z. Feng. *Eur. Polym. J.* 2005, **41**, 948–957.
17 D. Chimene, R. Kaunas, A.K. Gaharwar. *Adv. Mater.* 2020, **32**, 1902026.
18 L. Xiaorui, Z. Fuyin, W. Xudong, G. Xuezheng, Z. Shudong, L. Hui, D. Dandan, L. Yubing, W. Lizhen, F. Yubo. *Int. J. Bioprint.* 2022, **9**, 649.
19 S. Boularaoui, G. Al Hussein, K.A. Khan, N. Christoforou, C. Stefanini. *Bioprinting* 2020, **20**, e00093.
20 A. Torchio, M. Boffito, A. Gallina, M. Lavella, C. Cassino, G. Ciardelli. *J. Mater. Chem. B* 2020, **8**, 7696–7712.
21 A. Torchio, C. Cassino, M. Lavella, A. Gallina, A. Stefani, M. Boffito, G. Ciardelli. *Mater. Sci. Eng. C* 2021, **127**, 112194.
22 M. Boffito, F. Di Meglio, P. Mozetic, S.M. Giannitelli, I. Carmagnola, C. Castaldo, D. Nurzynska, A.M. Sacco, R. Miraglia, S. Montagnani, N. Vitale, M. Brancaccio, G. Tarone, F. Basoli, A. Rainer, M. Trombetta, G. Ciardelli, V. Chiono. *PLoS ONE* 2018, *13*, e0199896.
23 M. Boffito, E. Gioffredi, V. Chiono, S. Calzone, E. Ranzato, S. Martinotti, G. Ciardelli. *Polym. Int.* 2016, **65**, 756–769.
24 M. Boffito, A. Torchio, C. Tonda-Turo, R. Laurano, M. Gisbert-Garzarán, J.C. Berkmann, C. Cassino, M. Manzano, G.N. Duda, M. Vallet-Regí, K. Schmidt-Bleek, G. Ciardelli. *Front. Bioeng. Biotechnol.* 2020, **8**, 384.
25 C. Pontremoli, M. Boffito, S. Fiorilli, R. Laurano, A. Torchio, A. Bari, C. Tonda-Turo, G. Ciardelli, C. Vitale-Brovarone. *Chem. Eng. J.* 2018, **340**, 103–113.
26 M. Ding, J. Li, H. Tan, Q. Fu. *Soft Matter* 2012, **8**, 5414.
27 J. Hu, L. Tan. Polyurethane composites and nanocomposites for biomedical applications. In *Polyurethane Polymers*; Elsevier, 2017; pp 477–498.
28 R. Laurano, M. Boffito, M. Abrami, M. Grassi, A. Zoso, V. Chiono, G. Ciardelli. *Bioact. Mater.* 2021, **6**, 3013–3024.

View Article Online
DOI: 10.1039/D4TB00092G

29 H.H. Tønnesen, M. Másson, T. Loftsson. *Int. J. Pharm.* 2002, **244**, 127–135.
30 H.H. Tønnesen, J. Karlsen. *Z Lebensm Unters Forsch* 1985, **180**, 402–404.
31 Y. Nimiya, W. Wang, Z. Du, E. Sukamtoh, J. Zhu, E. Decker, G. Zhang. *Mol. Nutr. Food Res.* 2016, **60**, 487–494.
32 M. Kharat, Z. Du, G. Zhang, D.J. McClements. *J. Agric. Food Chem.* 2017, **65**, 1525–1532.
33 M. Wright, K. Kurumada, B. Robinson. Rates of incorporation of small molecules into pluronic micelles. In *Trends in Colloid and Interface Science XVI*; Miguel, M., Burrows, H. D., Eds.; Springer Berlin Heidelberg: Berlin, Heidelberg, 2004; pp 8–11.
34 X.J. Loh, L.W.I. Cheng, J. Li. *Macromol. Symp.* 2010, **296**, 161–169.
35 L. Wu, L. Yu, X. Fu, Z. Li. *Chin. J. Polym. Sci.* 2015, **33**, 1140–1149.
36 R. Laurano, V. Chiono, C. Ceresa, L. Fracchia, A. Zoso, G. Ciardelli, M. Boffito. *Eng. Reg.* 2021, **2**, 263–278.
37 J.W. Chung, T.J. Kang, S.Y. Kwak. *Macromolecules* 2007, **40**, 4225–4234.
38 C. Pradal, K.S. Jack, L. Grøndahl, J.J. Cooper-White. *Biomacromolecules* 2013, **14**, 3780–3792.
39 K.J. Henderson, T.C. Zhou, K.J. Otim, K.R. Shull. *Macromolecules* 2010, **43**, 6193–6201.
40 V. Kant, A. Gopal, D. Kumar, N.N. Pathak, M. Ram, B.L. Jangir, S.K. Tandan, D. Kumar. *J. Surg. Res.* 2015, **193**, 978–988.
41 S. Khan, M.U. Minhas, M. Ahmad, M. Sohail. *J. Biomater. Sci. Polymer Edition* 2018, **29**, 1–34.
42 R.S. Stowers, S.C. Allen, L.J. Suggs. *Proc. Natl. Acad. Sci. USA* 2015, **112**, 1953–1958.
43 A. Domiński, T. Konieczny, P. Kurcok. *Materials* 2019, **13**, 133.
44 A. Schwab, R. Levato, M. D'Este, S. Piluso, D. Eglin, J. Malda. *Chem. Rev.* 2020, **120**, 11028–11055.
45 H. Cao, L. Duan, Y. Zhang, J. Cao, K. Zhang. *Sig. Transduct. Target. Ther.* 2021, **6**, 426.
46 W.L. Ng, V. Shkolnikov. *Int. J. Bioprint.* 2024, 2135. https://doi.org/10.36922/ijb.2135.
47 W.L. Ng, J.M. Lee, M. Zhou, Y.W. Chen, K.A. Lee, W.Y. Yeong, Y.F. Shen. *Biofabrication* 2020, **12**, 022001.

Data availability

View Article Online
DOI: 10.1039/D4TB00092G

All relevant data are within the manuscript and the supporting information. The data are available from the corresponding author on reasonable request.